

MS No. M-2018-524.R1

Pyrrhotite Epidemic in Eastern Connecticut: Diagnosis and Prevention

by Dipayan Jana

Extensive cracking in thousands of residential concrete foundations in eastern Connecticut is found to be due to two-stage expansions associated with oxidation of pyrrhotite in crushed gneiss coarse aggregate of concrete used from a local quarry that sits on a hydrothermal vein of significant pyrrhotite crystallization, followed by internal sulfate attack in concrete from the sulfates released by pyrrhotite oxidation. Microstructural, chemical, and mineralogical evidences of pyrrhotite oxidation and the resultant internal sulfate attack in concrete are presented from a case study. A five-step laboratory testing protocol is suggested for assessment of aggregates from the area to prevent pyrrhotite-related deterioration for future construction.

Keywords: cracking; durability; oxidation; petrography; pyrrhotite; sulfate attack.

INTRODUCTION

Pyrite (FeS_2 , 46.6% Fe and 53.5% S) and pyrrhotite (Fe_{1-x}S , $0 < x < 0.125$, polytypes Fe_7S_8 , Fe_9S_{10} , $\text{Fe}_{11}\text{S}_{12}$) are two common iron sulfide minerals that occur as minor accessory minerals in many igneous, sedimentary, and metamorphic rocks.¹ Pyrite also occurs as a major phase in many sulfide ore bodies, and pyrrhotite as a secondary mineral in high-temperature hydrothermal and replacement veins, occurring often after pyrite, and with other iron sulfides—for example, pentlandite ($(\text{Fe,Ni})_9\text{S}_8$), marcasite (orthorhombic FeS_2), magnetite (Fe_3O_4), and chalcopyrite (CuFeS_2). Pyrite is a cubic-structured isotropic mineral with a yellowish-white color in reflected light and a characteristic metallic luster.¹ Pyrrhotite is a monoclinic (stable below 254°C) or hexagonal (stable above 254°C) anisotropic mineral with a pink-cream or skin color in reflected light that has a metallic luster and bronze-brown, yellow, or reddish color [Greek *pyrrhos*—flame-colored or redness¹]. Pyrrhotite is distinguished by its bronze rather than brass color of pyrite,¹ its lower hardness, decomposition in HCl with the evolution of H_2S ,¹ lower S/Fe ratio (0.50 to 0.65 as opposed to 1.15 in pyrite), and weakly magnetic nature. X-ray diffraction analysis determines the presence and amount of pyrite and pyrrhotite contents in a rock, whereas complimentary X-ray fluorescence analysis determines the total sulfur (as SO_3) content contributed from all iron sulfide minerals.

Concrete aggregates containing these iron sulfide species are known to cause various deteriorations from: a) unsightly stains, popouts of near-surface unsound aggregates, and associated local fracturing from oxidation of iron sulfide minerals in the presence of moisture and oxygen to, and b) in extreme cases, severe cracking, microcracking, and loss of strength and structural stability of concrete when sulfates (as

sulfuric acid) released from the oxidation process react with cement hydration products resulting in expansive reactions from internal sulfate attacks.² Concerns regarding possible iron sulfide-related distress in a concrete structure require proper identification of the type(s) of iron sulfide mineral responsible for the distress, quantification of the unsound constituent(s), oxidation products, and microstructural and microchemical evidences of extent and relative roles of oxidation and internal sulfate attacks on concrete durability.

Table 1 summarizes literatures on occurrences of concrete distress around the world from oxidation of pyrrhotite, followed by a few well-known cases from pyrite-related distress. Pyrrhotite-related concrete deteriorations have been reported in Oslo, Norway in 1959³ from oxidation of monoclinic pyrrhotite in alum shale sedimentary rock used as aggregate; in the Trois-Rivières area in Quebec, Canada in 2005^{4,21} from pyrrhotite in anorthositic gabbro coarse aggregate; in a dam in Spain in 2014⁸ from pyrrhotite in schist aggregate; and in northeastern Connecticut from pyrrhotite in crushed gneiss coarse aggregate.² Almost all these distresses are contributed to the two-stage mechanism of (Fig. 1): a) primary expansions of unsound aggregates associated with oxidation of pyrrhotite or pyrite in the presence of oxygen, moisture, and high pH in concrete to form ferric oxy-hydroxides—for example, ferrihydrite [$\text{Fe}(\text{OH})_3$], goethite $\text{FeO}(\text{OH})$, and limonite—causing staining, popout, or cracking of the unsound aggregates and concrete, followed by b) secondary expansions from internal sulfate attacks by the sulfates released from pyrrhotite oxidation to cement hydration and carbonation products forming secondary ettringite and thaumasite, respectively, causing further cracking. Total sulfur (as SO_3) content of unsound aggregates varied from as low as 0.2% to as high as 6%, and pyrrhotite content showed even more variation—from less than 5% to higher than 75% by volume of all iron sulfides. Due to such variability in chemistry (sulfur content) and mineralogy (potentially deleterious pyrrhotite content), proper detection of: a) the type of iron sulfide phase(s) responsible for the distress in concrete by microscopy; b) their proportion (from XRD); c) composition (sulfur content from XRF); and d) ‘available’ sulfur that can be released by moisture in an oxygenated environment (from accelerated oxidation test) are important.

ACI Materials Journal, V. 117, No. 1, January 2020.

MS No. M-2018-524.R1, doi: 10.14359/51718059, received December 13, 2018, and reviewed under Institute publication policies. Copyright © 2020, American Concrete Institute. All rights reserved, including the making of copies unless permission is obtained from the copyright proprietors. Pertinent discussion including author's closure, if any, will be published ten months from this journal's date if the discussion is received within four months of the paper's print publication.

Table 1—Case studies of concrete deterioration around the world due to oxidation of pyrrhotite and pyrite in unsound aggregates

Locality ^(Reference)	<ul style="list-style-type: none"> • Pyrrhotite-containing rocks • Associated sulfide minerals 	<ul style="list-style-type: none"> • Average sulfur content in aggregate • Pyrrhotite content 	<ul style="list-style-type: none"> • Structure affected • Type of damage • Time taken to manifest damage 	Proposed mechanisms of distress
Pyrrhotite-related deteriorations				
Oslo, Norway ³	<ul style="list-style-type: none"> • Sedimentary rocks (alum shales, some with slight metamorphism) • Pyrite was associated with pyrrhotite 	<ul style="list-style-type: none"> • 6% (highly variable), all shales that weathered ‘explosively’ due to oxidation contained more than 0.2% sulfur as monoclinic pyrrhotite. • Pyrrhotite content is related to rate of alteration of pyrite and rate of weathering of shale 	<ul style="list-style-type: none"> • Foundation • Upheaval of foundation, cracking, crumbling, yellowish deposit of jarosite [KFe₃(OH)₆(SO₄)₂] and brown-iron oxide (Fe₂O₃ · nH₂O) on weathered shales. • Within 9 months 	Swelling of shale due to oxidation of pyrrhotite and internal sulfate attack from released sulfate; reactivity of alum shale and resultant damage increased with increasing pyrrhotite content with no occurrence of damage when alum shale was free of pyrrhotite; acidic and sulfate-rich water percolated through alum shale has caused acid attack and internal sulfate attack in concrete.
Trois-Rivières area, Quebec, Canada ⁴⁻⁷	<ul style="list-style-type: none"> • Quarried intrusive igneous rock anorthositic gabbro (norite) with different degrees of metamorphism • Pyrite and chalcopyrite. Only pyrrhotite showed signs of oxidation but pyrite and chalcopyrite were largely unaffected. A thin coating of iron carbonate (siderite) on sulfides provided carbonates to promoted thaumasite form of attack in addition to internal sulfate attack from pyrrhotite oxidation 	<ul style="list-style-type: none"> • As low as 0.30% to 2.92% total sulfur by mass of aggregate in pyrrhotite-bearing coarse aggregates that have caused damage, all damaged concrete exceeded the European limit of 0.1% sulfur in aggregate when pyrrhotite is present by three times to as high as 30 times. • Less than 5 to 10% total sulfide minerals by volume, average 75% of sulfide minerals was pyrrhotite and lesser pyrite and chalcopyrite from a study of 223 house basements containing varying amounts of iron sulfide in gabbro coarse aggregate 	<ul style="list-style-type: none"> • Residential foundations and commercial buildings. • Map cracking (cracks up to 40 mm in width) and yellowish or brownish staining), popouts of oxidized pyrrhotite with white rim of secondary reaction products, and open cracks more pronounced at the corners of the foundation blocks • More than 1000 to as high as estimated 4000 residential and commercial buildings were affected within 3 to 5 years after construction 	Oxidation of sulfide minerals (mainly pyrrhotite) in anorthositic gabbro coarse aggregate in concrete has: a) formed various “rust” minerals (for example, ferric oxyhydroxides such as goethite FeO(OH), limonite, and ferrihydrite); and b) released sulfuric acid/sulfates, which then reacted with cement hydration products resulting in further expansive formation of gypsum, ettringite, and thaumasite in concrete. Oxidation of pyrrhotite, followed by internal sulfate attack of cement paste are the main mechanisms of concrete deterioration.
Northeastern Connecticut ²	<ul style="list-style-type: none"> • Foliated schist and gneissic metamorphic rocks, granofels, foliated quartz diorite in a hydrothermally altered vein from a particular quarry in Willington, CT (Becker’s quarry). • Pyrrhotite as the predominant iron sulfide mineral present in metamorphic rocks containing quartz, plagioclase feldspar, micas, and garnet 	<ul style="list-style-type: none"> • Average 2.54% sulfur in pyrrhotite-bearing quarry aggregate • Pyrrhotite was not detected in XRD analysis of quarry aggregate by Wille and Zhong due to possible presence below the detection limit of XRD 	<ul style="list-style-type: none"> • Residential foundations. • Map cracking, crumbling, deformation of wall, reddish-brown discoloration, whitish formation of secondary ettringite and thaumasite in the vicinity of surface cracks. Cores from foundation walls of houses showed noticeably lower compressive strengths (some no strength due to complete crumbling) compared to the cores from slabs, indicating possible effect of more oxidation in wall than slab and hence more damage in wall than slab • 10 to 20 years after construction, estimated 34,000 homes are at risk 	Primary expansion due to oxidation of pyrrhotite, followed by secondary expansion due to internal sulfate attack by the released sulfates.
Catalan Pyrenees, Spain ⁸⁻¹⁰	<ul style="list-style-type: none"> • Schist containing quartz, muscovite mica, chlorite and non-expansive illitic clay. • Pyrite and Pyrrhotite 	<ul style="list-style-type: none"> • 2% sulfur (as SO₃ from XRF) in schist. • Predominantly pyrrhotite (S/Fe ratio 0.62 as opposed to 1.15 of pyrite) but XRD also detected some pyrite 	<ul style="list-style-type: none"> • Tórán Dam • Map cracking and non-recoverable movements, more dramatic expansion in the downstream face of the dam for upstream displacement of the crest 	Oxidation of pyrite and pyrrhotite forming surface stains of greyish brown iron hydroxides (goethite) and lighter-green potassium iron sulfates (jarosite), gypsum efflorescence from sulfate attack; and causing expansions—for example, 6.04 cm ³ /mol from primary expansion from oxidation of iron sulfides followed by 172.19 cm ³ /mol from internal sulfate attack by reaction between released sulfates and cement phases

Table 1 (cont.)—Case studies of concrete deterioration around the world due to oxidation of pyrrhotite and pyrite in unsound aggregates

Central Pyre- nees, Spain ^{11,12}	<ul style="list-style-type: none"> • Schist containing bands of pyrrhotite that created planes of weakness and present cracks that serve as preferential paths for entrance of oxygen thus aggregates containing pyrrhotite bands with cracks showed much more pronounced oxidation than the aggregates without cracks. • Pyrite 	<ul style="list-style-type: none"> • Median sulfur (SO₃) content of 1.42% for rocks from a quarry that have known to cause severe damage when used as aggregate in dam 	<ul style="list-style-type: none"> • Graus and Tavascan Dams • Map cracking, damage in downstream face and galleries of the Graus Dam due to severe cracking and movement 	Alteration from acidic solution produced by weathering and oxidation of pyrrhotite in aggregates followed by expansion due to internal sulfate attack and formation of ettringite and gypsum. Characteristic ratios of 2.44 for the Fe/O ratio and of 2.63 for the S/O ratio in pyrrhotite marked critical limits that produced the activation and acceleration of pyrrhotite oxidation leading to an increase of expansive reactions and risk of structural damage.
---	--	--	---	--

Pyrite-related deteriorations

<ul style="list-style-type: none"> • Ottawa, Quebec City, Matane, and Montreal, Canada¹³⁻¹⁶ • Ireland • Wales¹⁷ • Marcellus Shale, U.S.¹⁸ • Chattanooga Shale, Kentucky¹⁹ • SW England in Cornwall and Devon 	<ul style="list-style-type: none"> • Black shale containing pyrite (not pyrrhotite). Pyrite was most common in shale as either a primary mineral or a fine, wide-spread impregnation of subsequent origin. • Pyrite is frequently found in association with coal and shale deposits • Mundic (mine waste) concrete blocks used in the foundations of thousands of twentieth century homes in SW England, blocks were prepared using mine waste rocks as aggregates containing pyrite that has caused serious damage (Mundic decay) in foundations 	The minimum amount of pyrite that has caused heaving problems was not known with certainty. Some reports described difficulties with pyrite contents as low as 0.1% by weight. In the Ottawa area, heaving problems have been encountered only in rock formations with much higher pyrite contents, although a systematic sampling program has not been carried out. Pyrite weathering is a chemical-micro-biological oxidation process; some of the oxidation reactions are solely chemical, others are attributed to autotrophic bacteria of the ferrobacillus-thiobacillus group, and still others are both chemical and microbiological.	<ul style="list-style-type: none"> • Foundation, basement floor above weathered pyritic substrate. Pyrite weathering was identified as early as 1950 as a major foundation problem in the U.S. in buildings dating back to 1920. • Pyrite oxidation in the Chattanooga Shale has caused serious foundation problems in numerous buildings and structures in Estill County, KY. • Heaving of pyritic substrate causes cracking, lifting of concrete floor slabs; differences in levels across floor slabs; cracking, buckling, lifting of elements resting on the concrete floor slabs, doors, stairs, fixtures; cracking, bulging, movement of internal or external walls. • Blistering and de-bonding of vinyl tile from concrete floor is reported due to oxidation of pyritic aggregates at the surface of concrete floor²⁰ 	Oxidation of pyrite in shale or coal has caused formation of <i>gypsum</i> from reactions between: a) sulfates or sulfuric acid released from pyrite oxidation and calcium hydroxide component of cement hydration (if pyritic rock is used as aggregate in concrete); and/or b) between sulfuric acid from oxidation and associated calcite in pyritic rocks cause heaving and associated volume changes. When calcite converts to gypsum, the volume increases by a factor of 2, but of greater importance is the force associated with the growth of gypsum crystals, which can be very high. When gypsum grows in rock under buildings it tends to form needle-like crystals that force the layers apart, resulting in much greater heave than would occur with simple volume expansion during formation. Another oxidation product found in all weathered pyritic materials is jarosite, KFe ₃ (SO ₄) ₂ (OH) ₆ , recognized by its bright yellow-brown color. The calculated volume increase from pyrite to jarosite is 115%, which was another main contributor to volume increase and heaving.
--	--	--	---	--

RESEARCH SIGNIFICANCE

Widespread cracking and crumbling of many residential concrete foundations in northeastern Connecticut has affected over 600 homes at the time of this report with an estimated replacement cost of foundations ranging from \$150,000 to \$250,000 per home, along with more serious concern for an additional estimated 35,000 homes across 41 towns in the north, east, and central parts of Connecticut that have reportedly received concretes made using unsound aggregate from the same supplier.^{22,23} Most of the damages to date have been linked to aggregates supplied from one quarry (Becker’s quarry) in Willington, CT, operated during 1980s for 30 years that sits in a weathered hydrothermal vein of metamorphic rocks containing significant pyrrhotite mineralization. The geology in the vicinity of the quarry is made up of metamorphic rocks predominately from two to three formations, consisting mainly of foliated schists and gneissic rock, granofels, and foliated quartz diorite.²⁴ Quartz and feldspar are the primary minerals along with

micas (biotite), garnet, and pyrrhotite as common accessory minerals. The cause of deterioration has been attributed to expansions from oxidation of pyrrhotite present as the predominant iron sulfide, followed by internal sulfate attack in paste from the released sulfates² with manifestation of the damage that has taken as many as 10 to 20 years to appear. Typical visual forms of deterioration (Fig. 2) are map cracking of foundation walls, some causing deformation of the walls, reddish-brown discoloration as rust stains, whitish formation of sodium sulfate salts (thenardite and mirabilite) in the vicinity of surface cracking, and, in severe cases, crumbling of foundation.²

CASE STUDY AND METHODOLOGIES

In light of this known problem of pyrrhotite in concrete aggregate from around the world, and particularly from Becker’s quarry, and the resulting distress in many residential foundations in northeastern Connecticut, map cracking and reported crumbling of one such residential foundation

Concrete deterioration is due to: (1) primary expansion of unsound aggregates from oxidation of iron sulfide + (2) secondary expansion of released sulfate-contaminated paste due to internal sulfate attack (formation of poorly-crystallized ettringite in the confined spaces in paste some of which becomes well-crystallized in open voids, cracks, and aggregate-paste interfaces)

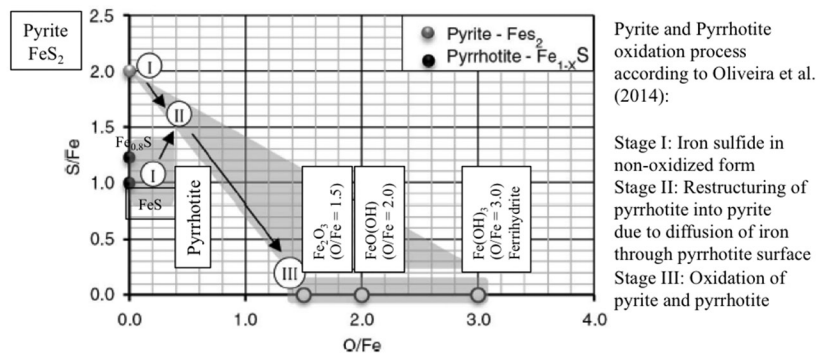
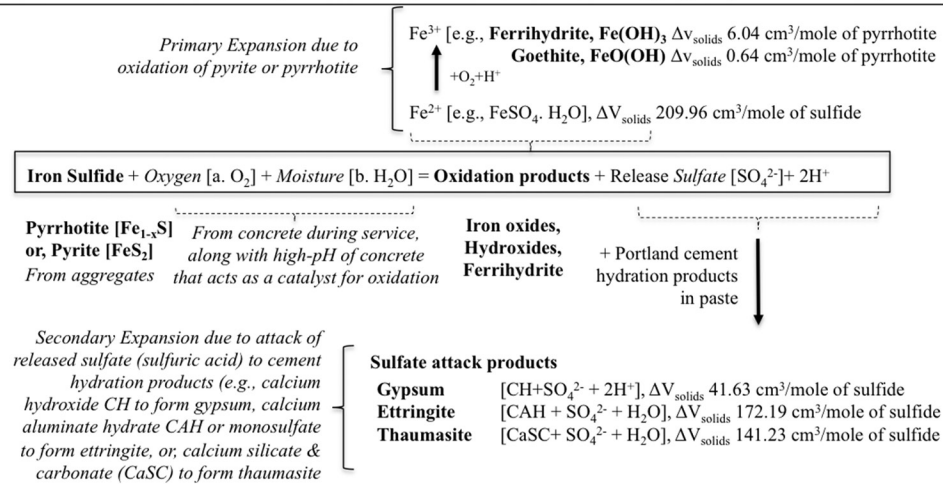


Fig. 1—Mechanisms of concrete deterioration by oxidation of iron sulfide minerals in aggregates (after Wille and Zhong² and Oliveira et al.¹²). Increases in solid volumes (ΔV_{Solid}) from oxidation of pyrrhotite to ferrihydrite through an intermediate state of Fe^{2+} ($\text{FeSO}_4 \cdot \text{H}_2\text{O}$), followed by further solid volume increases from internal sulfate attacks of sulfates to cement hydration products and formation of calcium sulfate hydrate (gypsum), sulfoaluminate hydrate (ettringite), and silicate-carbonate hydrate (thaumasite) cause deteriorations in concrete.

wall in Ellington, CT—that is, within the known location of ‘pyrrhotite epidemic’—has steered the concern of: a) whether or not the deteriorated concrete foundation contained pyrrhotite in its aggregate; and, if detected, b) whether pyrrhotite has played the primary role for the observed cracking and crumbling as suspected in other cracked foundations from the area.

After field survey of cracks in the foundation, a 10 in. long, 4 in. diameter concrete core drilled from over a visible map crack through the entire thickness of the foundation wall was retrieved for laboratory testing (Fig. 3). Detection of pyrrhotite, along with overall condition of concrete and pyrrhotite-bearing aggregates were examined by detailed petrographic examinations according to the methods of ASTM C856²⁶ starting with optical microscopy from: a) low-power (up to 100 \times) stereo-microscopical examinations of as-received core, saw-cut, lapped, and fluorescent-dye impregnated cross sections of core; to b) examinations in a high-power (up to 600 \times) petrographic microscope of multiple polished, blue dye-mixed epoxy-impregnated thin sections (30 micron thick, 50 x 75 mm size) prepared from one end of the core (wall) to the other. Impregnating concrete with a

low-viscosity epoxy mixed with a fluorescent dye for lapped cross sections and a blue dye for thin sections highlighted many fine hairline microcracks more vividly when viewed in reflected ultraviolet (UV) light and transmitted polarized light, respectively, than were otherwise visible without such impregnations. Understanding deleterious roles of pyrrhotite, its composition and oxidation products, sulfate levels of paste from internal sulfate attack, and microstructures of deteriorated concrete around pyrrhotite-bearing aggregates required further examination by scanning electron microscopy and microanalysis by energy-dispersive X-ray fluorescence spectroscopy (“SEM-EDS” according to the methods of ASTM C1723²⁷) of thin sections already examined in petrographic microscope to select areas of interest for SEM-EDS study. X-ray diffraction (“XRD” according to the methods of ASTM C1365²⁸) and X-ray fluorescence (XRF) of multiple pyrrhotite-bearing coarse aggregate particles, carefully extracted from the concrete by removing the adhered paste and ground to finer than 0.045 mm particle size to form pressed pellets, provided the pyrrhotite content, its oxidation products, and total sulfur (as SO₃) content of aggregate. Anion exchange chromatography (according to

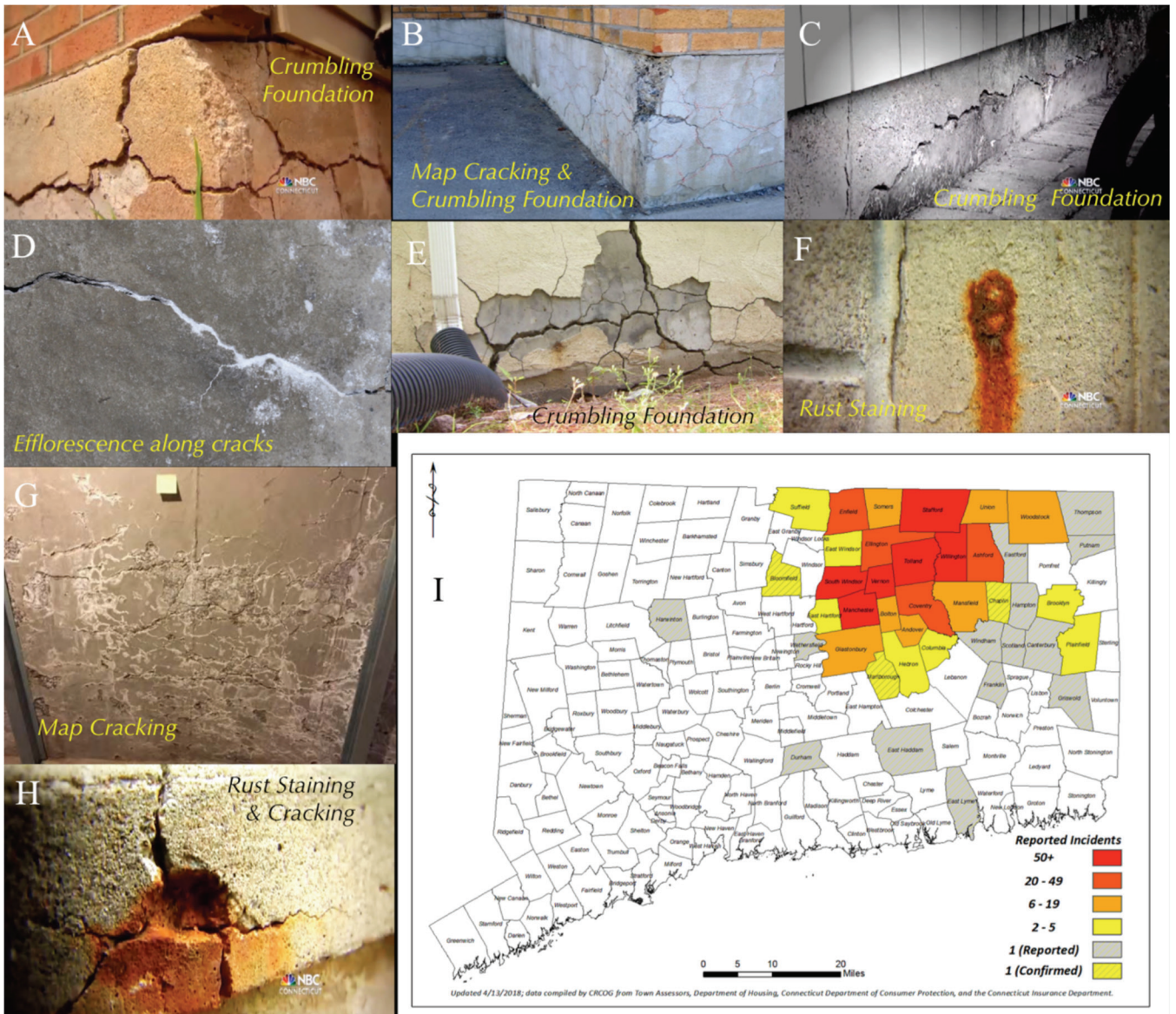


Fig. 2—Cracking in residential foundations from eastern Connecticut due to pyrrhotite-related deterioration of concrete. Photo credits: NBC Connecticut for photos A, B, C, D, F, and H; Wille and Zhong² for photo G; and Capitol Region Council of Governments (CROG) for photo E.²⁵ Photo I shows a map of northeastern Connecticut compiled at the time of preparation of this article by CROG from Town Assessors, Department of Housing, Connecticut Department of Consumer Protection, and Connecticut Insurance Department where townships having very high incidences (50+) of pyrrhotite-related distress, as well as the ones having high (20 to 49), medium (6 to 19), and low (2 to 5) incidences of distress are shown in various shades of colors.

the methods of ASTM D 4327²⁹) of filtrates of extracted aggregate particles pulverized to finer than 0.3 mm and digested in a strong oxidant—for example, of 35% hydrogen peroxide solution—for several days in an accelerated oxidation test then diluted in deionized water, provided rate and levels of sulfates released by these aggregates that are ‘available’ for internal sulfate attack in relation to a ‘control’ aggregate without any iron sulfide mineral.

OPTICAL MICROSCOPY

Optical microscopy determined the foundation concrete to be made using crushed stone coarse aggregate, natural siliceous sand fine aggregate, portland cement paste, and entrained air. Coarse aggregate (Fig. 4) is a mixture of a predominant dark gray metamorphic garnetiferous quartz-

zo-feldspathic and micaceous gneiss and a subordinate light brown quartz-feldspar-mica gneiss (having a higher quartz content than the dark gray gneiss) both having a nominal maximum size of 3/4 in. (19 mm), showing the typical gneissose texture of alternating bands of quartz-albitic feldspar and micaceous (mostly biotite and less muscovite) minerals that often contain anhedral garnet poikiloblast (Fig. 5 and 6). It is well-graded (similar to the grading requirements of ASTM C33 for No. 6 size coarse aggregate) and well-distributed. Fine aggregate has a nominal maximum size of 3/8 in. (9.5 mm) and contains major amounts of quartz and quartzite, and subordinate amounts of feldspar, mica, ferruginous rock, and mafic minerals. Portland cement was used as the sole cementitious component, having an estimated cement content of 6 to 7 bags/yd³ and an estimated

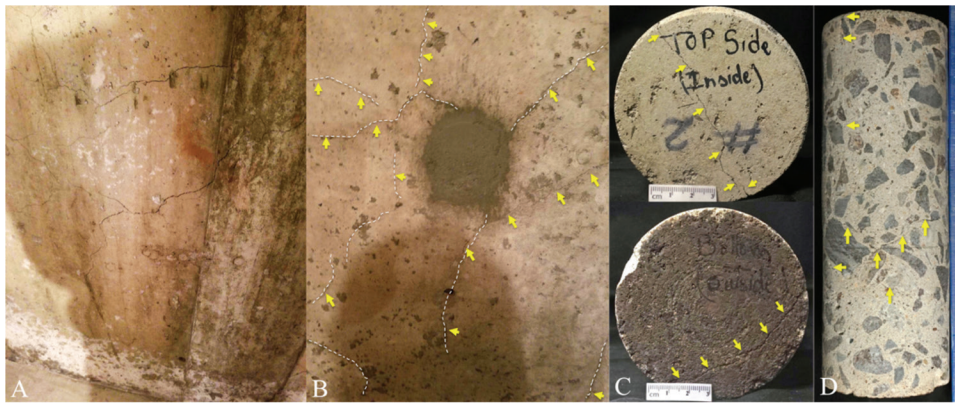


Fig. 3—The 10 in. long concrete core collected from the entire thickness of a cracked residential foundation wall in Ellington, CT examined in this study. Arrows show visible cracks on the foundation wall as well as on the surfaces of core retrieved from over one such crack.

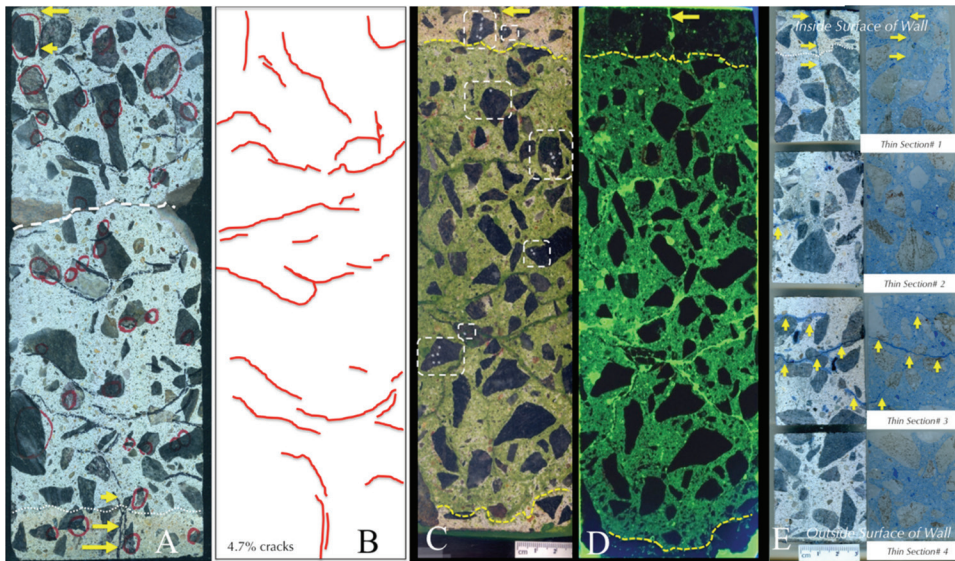


Fig. 4—From left to right: (A) Lapped through-wall cross section of core showing: (i) extension of visible cracks from the inside and outside surfaces of wall (arrows); (ii) extension of cracks throughout entire thickness of core (highlighted by black lines); (iii) occurrences of iron sulfide minerals in dark crushed stone aggregates (many are circled); and (iv) approximately 20 mm deep carbonation from the inside wall surface as shown by beige discoloration of concrete at the bottom end of cross section (carbonated zone is separated from interior concrete by a white dotted line); (B) Traces of cracks in the left cross section; (C) A second through-wall lapped cross section, sectioned parallel to the first one and impregnated with a low-viscosity fluorescent epoxy to highlight the network of cracks when viewed in UV light as shown in (D). Dark aggregate particles containing iron sulfide minerals (marked in silver dots on aggregate) are marked in dashed boxes in (C). The inside end of foundation wall is at the top ends of the photos in (C) and (D) that shows 40 mm deep carbonation. Carbonated zone is separated from non-carbonated interior by dashed lines. Carbonation-induced beige discoloration of paste is noticed in (C), and carbonation-induced densification of paste is best seen in (D) due to noticeably lower absorption of fluorescent dye in carbonated paste compared to the non-carbonated interior. E shows blue dye-mixed epoxy-impregnated thin sections prepared from a third cross section of core sectioned parallel to the ones shown in (A) and (C), and after impregnating the third cross section in vacuum with a blue dye-mixed epoxy to highlight cracks and voids.

water-cement ratio (w/c) of 0.45 to 0.50. Cement paste was carbonated to a distance of 40 to 50 mm from the inside wall, and, 20 to 30 mm from the outside wall surface, with extensive microcracking many of which originated from cracked gneiss coarse aggregate particles. The concrete was air-entrained, having an estimated air content of 6 to 7%.

Optical microcopy traced visible cracks on the foundation walls from surface inward and found the cracks extended throughout the entire thickness of the wall (Fig. 4). Cracks

are random, up to 1 mm in width, tapered down from the wall surfaces to depths of 20 to 50 mm (at least in the core examined), transected and/or circumscribed the crushed gneiss coarse aggregate particles, and showed a pattern that cannot be formed by typical concrete shrinkage or settlement of the wall but more likely by chemical deterioration in line with the suspected expansions from oxidation of pyrrhotite-bearing aggregates and subsequent internal sulfate attack by the released sulfates in concrete. Severe

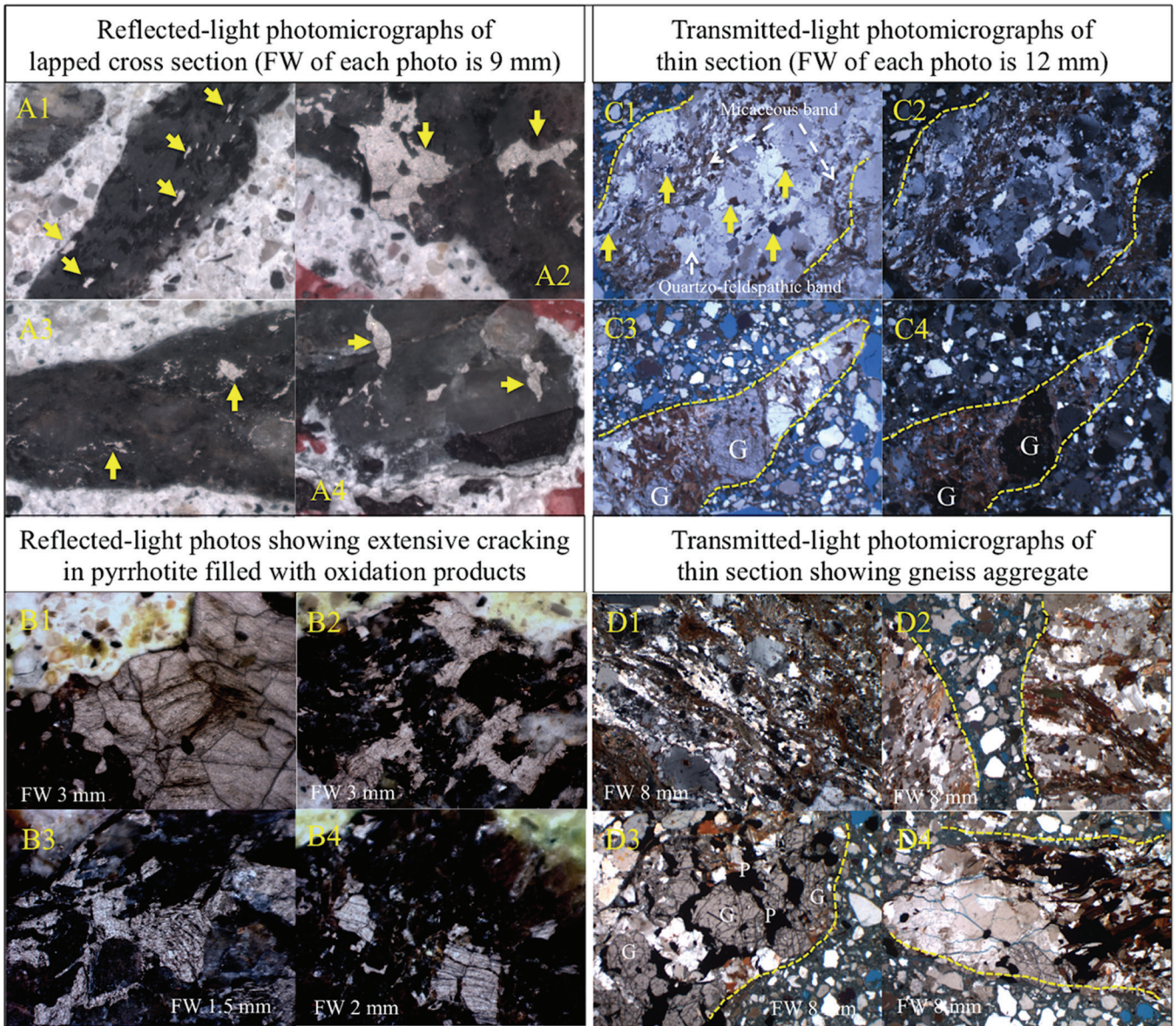


Fig. 5—Photomicrographs of lapped cross section taken from a reflected-light low-power stereomicroscope (A and B series), and, photomicrographs of thin section taken from a transmitted-light high-power Stereozoom microscope with polarized-light facilities (C and D series) showing: (a) disseminated iron sulfide grains in crushed gneiss coarse aggregate occurring either as fine metallic lustered pyrrhotite grains aligned along the gneissose planes of aggregate (A1, A3), or as coarser isolated grains (A2, A4); (b) extensive cracking in pyrrhotite inclusions in gneiss due to oxidation (B series); (c) garnetiferous quartz-feldspar-mica gneiss composition of aggregate (C and D series) that contains dark iron sulfide inclusions identified as pyrrhotite (arrows in C1); (d) alternating bands of quartzo-feldspathic and micaeous layers in gneiss (D1 and D2); (e) interlocking garnet (G) and pyrrhotite (P) grains in gneiss (D3); and (f) microcracking in gneiss due to pyrrhotite oxidation where microcracks are highlighted by blue epoxy (D4). (Note: FW is field width.)

cracking of the wall was the reason for reported crumbling of the foundation.

As mentioned, optical microscopy detected two types of crushed gneiss coarse aggregate particles (Fig. 4, 5, and 6): a) a dominant dark gray crushed gneiss that contains alternating bands of quartz-feldspar and micaeous (mostly biotite less muscovite) minerals (defining the gneissose texture) and pyrope garnet poikiloblast, and lesser quartz than the other; and b) less predominant light brown crushed gneiss. Both gneiss types contained iron sulfide minerals (more common in the predominant dark gray gneiss particles but

more cracked in the light brown gneiss particles [Fig. 5]) as small equant to irregular-shaped to elongated particles with characteristic metallic luster and optically semi-opaque natures (Fig. 5). Multiple lapped cross sections of core show many such iron sulfide inclusions mostly concentrated in the dark gray crushed gneiss and lesser in light brown coarse aggregate throughout the entire depths of the cross sections. Features like bronze color of pyrrhotite (rather than brass color of pyrite), lower hardness, decomposition in HCl, weakly magnetic nature, and reddish-brown oxidation products are helpful for detection of wide distribution

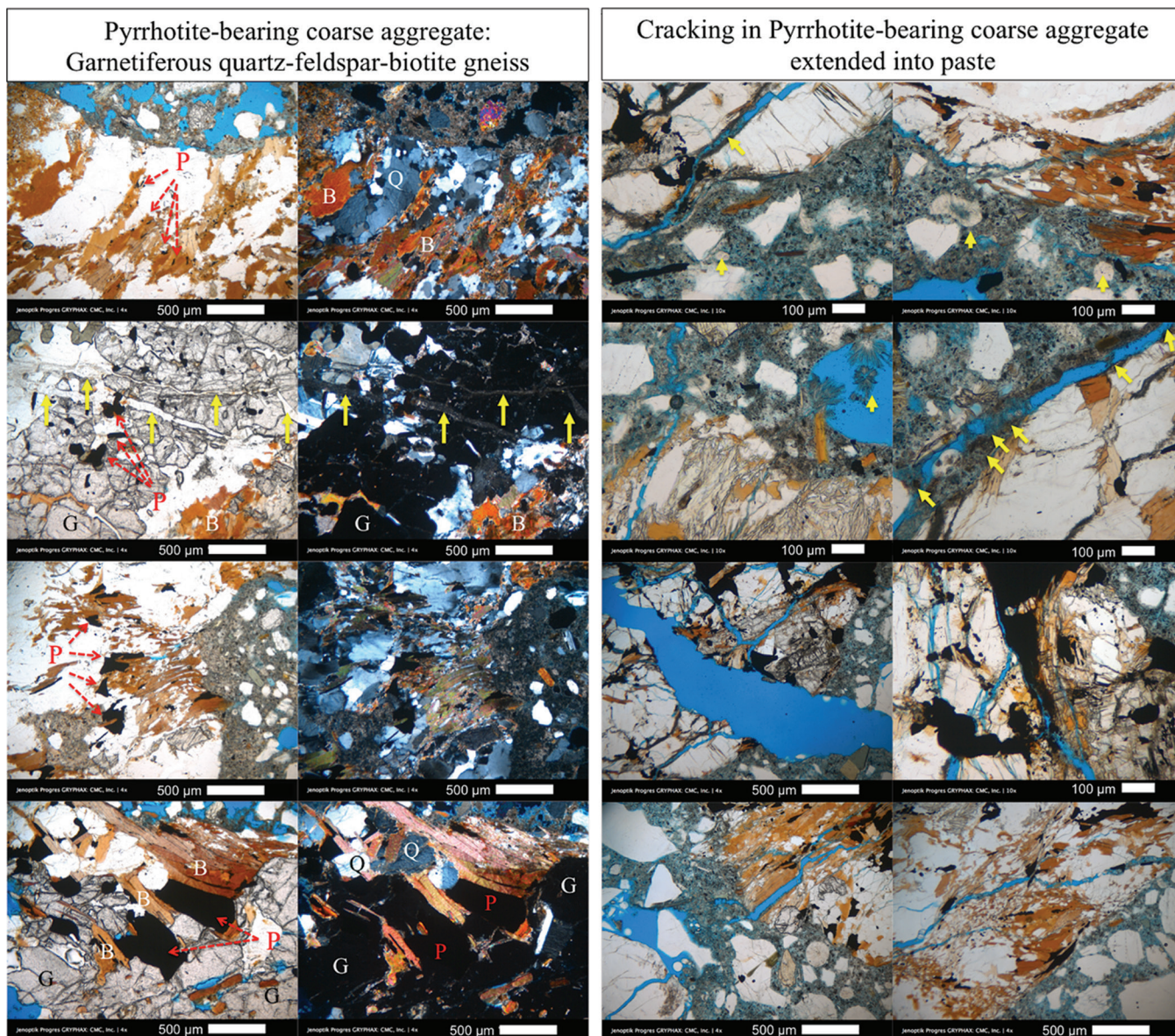


Fig. 6—Photomicrographs of blue dye-mixed epoxy-impregnated thin sections of concrete showing pyrrhotite-bearing garnetiferous quartz-feldspar-mica gneiss coarse aggregate in the left column of eight photos where each photo was taken in plane and corresponding crossed polarized light mode with a petrographic microscope. Scale bar in these eight photos represent 0.5 mm. Pyrrhotite inclusions (P) occur in variable grain sizes in quartz (Q), feldspar, biotitic mica (B), and garnet (G) minerals of gneiss. Extensive cracking of gneiss is seen in the second row of left column photos, which are shown more elaborately in eight photomicrographs in the right column, all of which were taken in plane polarized-light mode with a petrographic microscope (cracks are highlighted by blue epoxy, scale bars are mostly 0.1 mm in length).

of pyrrhotite grains in crushed gneiss aggregates. Abundant iron sulfide mineralization in hydrothermal vein, on which the subject quarry was situated and reportedly supplied the coarse aggregate, is established in the examined concrete. Similar pyrrhotite-bearing crushed gneiss coarse aggregates are found in many other foundations from northeast Connecticut that have shown pyrrhotite-oxidation-related cracking.

MICROSTRUCTURAL EVIDENCE OF DISTRESS

Visible (macro) and invisible (micro) cracking of pyrrhotite-bearing crushed gneiss aggregate from pyrrhotite oxidation, cracks often extending from unsound aggregates to paste, and reddish-brown stain of pyrrhotite oxidation prod-

ucts sometimes associated with unsound particles are the first telltale signs of distress. Microcracks in many affected gneiss particles followed the micaceous bands due to the internal plane of weakness in gneissose-textured rock (Fig. 6), defined by alternating layers of denser quartzo-feldspathic minerals and flaky biotitic mica, where later layer provided the planes of weakness (foliation) to develop cracking during expansions from oxidation of pyrrhotite. As a result, a lot of cracks within the gneiss coarse aggregate particles are found along the weak bands of mica flakes. In many particles, however, no such preferential path of cracking is noticed. Oliveira et al.¹² found pyrrhotites occurring as bands in plate-shaped geometry in schist that have

Innocuous & Deleterious Secondary Ettringite Formation from Moisture-Induced Internal Sulfate Attack in Paste By Sulfates Released From Oxidation of Pyrrhotite

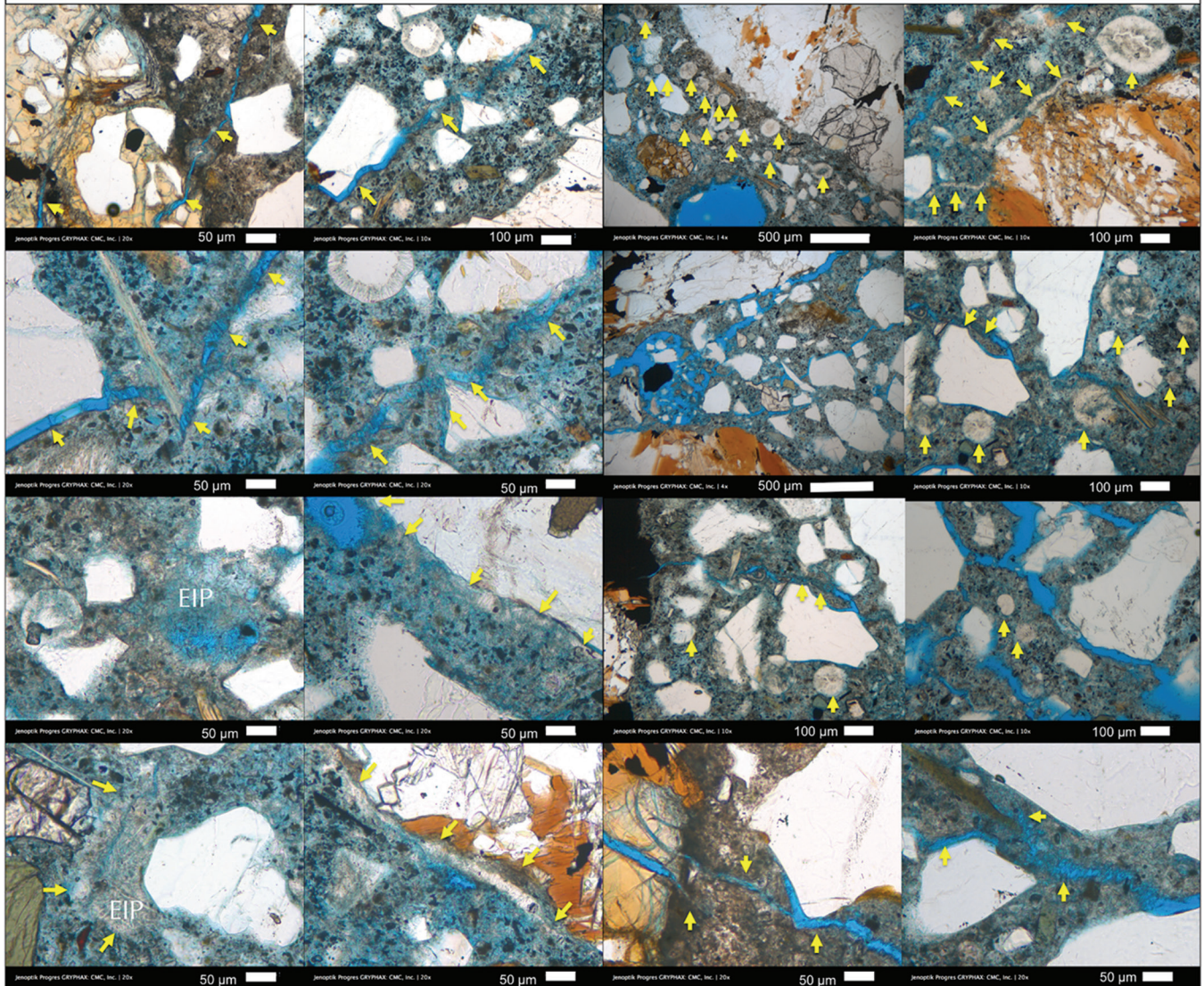


Fig. 7—Photomicrographs of blue dye-mixed epoxy-impregnated thin sections of concrete showing extensive secondary ettringite formation lining the walls of air voids, cracks (arrows show some such occurrences in voids and cracks), as well as ettringite intermixed with cement hydration products in confined areas of paste (marked as EIP or ettringite-infested paste).

created planes of weakness and cracks for the entrance of oxygen and, hence, enhanced oxidation.

The next microstructural evidence is abundant secondary ettringite crystallization lining or filling many air voids and occasionally lining some microcracks (Fig. 7) that are indicative of prolonged presence of moisture in concrete during service, which is an essential prerequisite for pyrrhotite oxidation. It also indicates availability of sulfates for secondary ettringite crystallization, which, however, may or may not have necessarily derived from pyrrhotite oxidation because ettringite-filled air-voids are a very common microstructural feature in a concrete exposed to moisture during service with or without iron sulfide contaminant.

SULFATE CONTENT OF CONCRETE FROM XRF

Establishing the sources of secondary ettringite, either from portland cement's sulfate and/or from oxidation of

pyrrhotite-bearing aggregates, requires determination of sulfate levels in concrete—namely, if the level is higher than that expected from a typical portland-cement concrete where sulfate (as SO_3) content in cement is usually around 3 weight percent, which gives approximately 0.45% sulfate in concrete for a usual cement content of 15% by mass of a normalweight concrete. Excess sulfate in concrete above 0.45% from cement's contribution would then correspond to the pyrrhotite-aggregate source if no other sulfate source is present. To determine the sulfate (SO_3) level of bulk concrete, a thin slice of concrete was sectioned through the entire length of the core traversing the full thickness of the foundation wall and pulverized for XRF analysis, which showed 1.45% bulk sulfate (SO_3) by weight of concrete, which is more than three times sulfate than that normally contributed from portland cement. Clearly, some of the secondary ettringite crystallization in air voids and microcracks were derived from

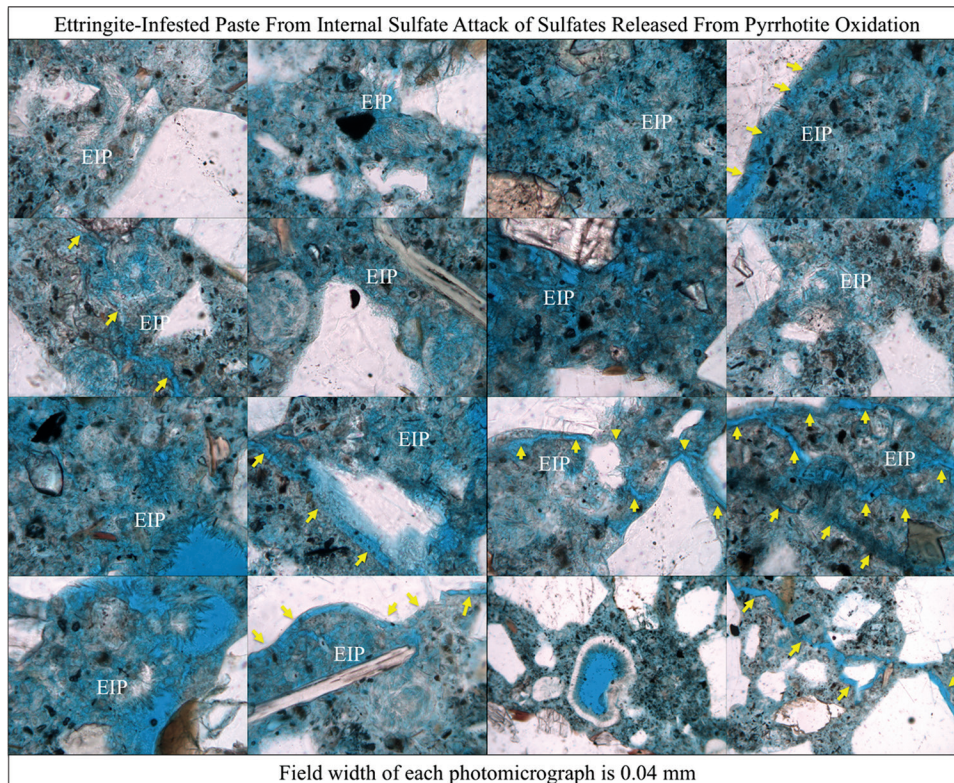


Fig. 8—A common microstructural feature of pyrrhotite-related distress in concrete is occurrences of microcrystalline to cryp-tocrystalline (and perhaps colloidal) form of ettringite intimately mixed with other cement hydration products that are more difficult to observe than secondary ettringite in voids and cracks (that are more easily visible by their fine acicular shape and optical properties). These ettringite-infested paste (marked as EIP in many photos above) regions are responsible for expansion and associated distress in concrete beyond the one from pyrrhotite oxidation-related expansion. All photomicrographs were taken in plane-polarized light mode with a petrographic microscope at a high magnification where fine, well-formed, acicular ettringite crystals are more visible in the porous areas of paste than microcrystalline ettringite in the denser ettringite-infested paste regions.

sulfates other than portland cement, having the most likely source from oxidation of pyrrhotite in coarse aggregate.

ETTRINGITE IN CEMENT PASTE

To establish secondary expansion of paste from internal sulfate attacks—that is, by reactions between sulfates released from pyrrhotite oxidation and cement hydration products—microstructural evidence for expansion of the sulfate-contaminated hydrated cement paste has to be established. A common microstructural evidence of paste expansion commonly attributed to delayed ettringite formation (DEF) in many steam-cured precast concrete elements is gaps or separations around aggregates due to direct expansion of paste relative to aggregate,³⁰ where widths of the gaps are usually proportional to the size of the aggregates.³⁰ Optical microscopy did not detect many such systematic gaps around aggregates, or similar features as found in many cracked precast concrete members deteriorated by DEF. Another feature common in sulfate attacks from internal or external sulfates is ettringite-filled cracks, which is seen in the present concrete, especially in the interior cracked regions. Therefore, the possibility of paste expansion from an internal sulfate attack by reactions between ‘excess’ (that is, beyond cement’s contribution) sulfates released from pyrrhotite oxidation and cement hydra-

tion products are diagnosed both by optical microscopy and subsequently by SEM-EDS.

The most interesting microstructural feature detected in the present concrete is poorly crystalline (perhaps some colloidal form) secondary ettringite formed in the confined areas of paste rather than the well-formed acicular or fibrous secondary ettringite commonly found in voids or cracks in a concrete exposed to moisture. The former type (poorly crystalline secondary ettringite in confined areas of paste) is described here forming in ettringite-infested paste (Fig. 8), which are judged to be the areas of internal sulfate attacks that have caused secondary expansion of paste and associated cracking. The main mechanism of paste expansion from internal sulfate attack is not so much due to precipitation of secondary ettringite in voids and cracks, but more due to expansions from formation of poorly crystalline (or colloidal) ettringite in relatively confined areas in paste, followed by further swelling by moisture absorption. Ettringite-lined voids or cracks are most commonly the result, not the cause, of internal sulfate attack, whereas poorly crystalline ettringite in confined areas of paste are the direct cause for expansion and cracking of paste and around aggregate-paste interfaces. Ettringite-infested paste is directly responsible for high sulfate content of paste, as detected in the subsequent SEM-EDS studies, which is

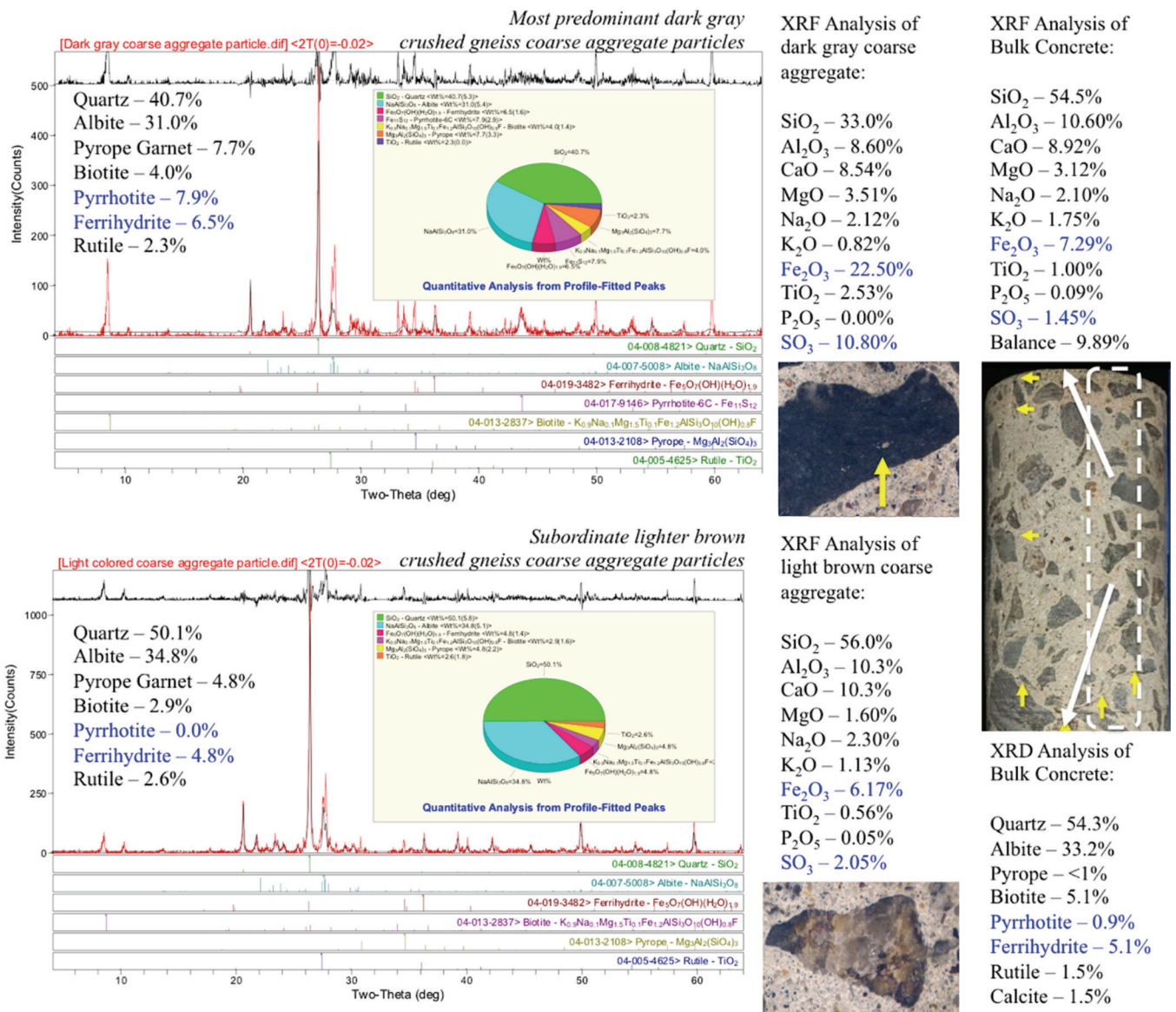


Fig. 9—X-ray diffraction patterns and quantitative (Rietveld) determination of minerals (in the inset values and in pie graphs) in a dark gray crushed gneiss at the top and a light brown crushed gneiss at the bottom showing variations in pyrrhotite and other minerals' contents between the two gneiss types. Also shown in the right column are compositional analyses of pressed pellets of these two aggregate particles as major element oxide compositions from an energy-dispersive X-ray fluorescent spectrometer. The last column shows XRD and XRF compositions of pressed pellet of a pulverized bulk concrete sectioned as a thin strip of approximately 6 mm thickness from the top to bottom end of core (marked as dashed white line in the core photo). In both aggregate particles, ferrihydrite is found as the oxidation product of pyrrhotite with remaining pyrrhotite still present in the dark gneiss particle but used up entirely in the light brown particle. Pyrrhotite content is as high as 8% in the dark gneiss and 0.9% in bulk concrete. Sulfate contents from XRF are 10.8% in dark gneiss, 2% in light brown gneiss, and 1.45% in bulk concrete.

the more powerful evidence for internal sulfate attack than simple secondary ettringite-filled voids and cracks.

XRD AND XRF OF UNSOUND AGGREGATE

XRD analyses of coarse aggregate particles extracted from the core have confirmed the iron sulfide minerals to be pyrrhotite, along with ferrihydrite as its oxidation product (Fig. 9), which are in line with previous findings from other deteriorated foundations.² XRD and XRF studies of two crushed gneiss types showed characteristic difference in mineralogy and chemistry between the darker and lighter

varieties—for example, having higher quartz in lighter brown particle, higher pyrrhotite in darker gray particles, and higher iron oxide and sulfate in dark gray particle in XRF. As high as 10.8% sulfur (as SO₃) is detected in a dark gray crushed gneiss coarse aggregate particle, which is 10 times higher than the minimum 1.0% SO₃ limit by mass of aggregates established in many codes and guidelines. Light brown crushed gneiss showed 2.0% sulfur. XRD analyses showed as high as 8% pyrrhotite in the predominant dark gray crushed gneiss coarse aggregate but none in a light brown one; both types showed 4.8 to 6.5% ferrihydrite (Fig.

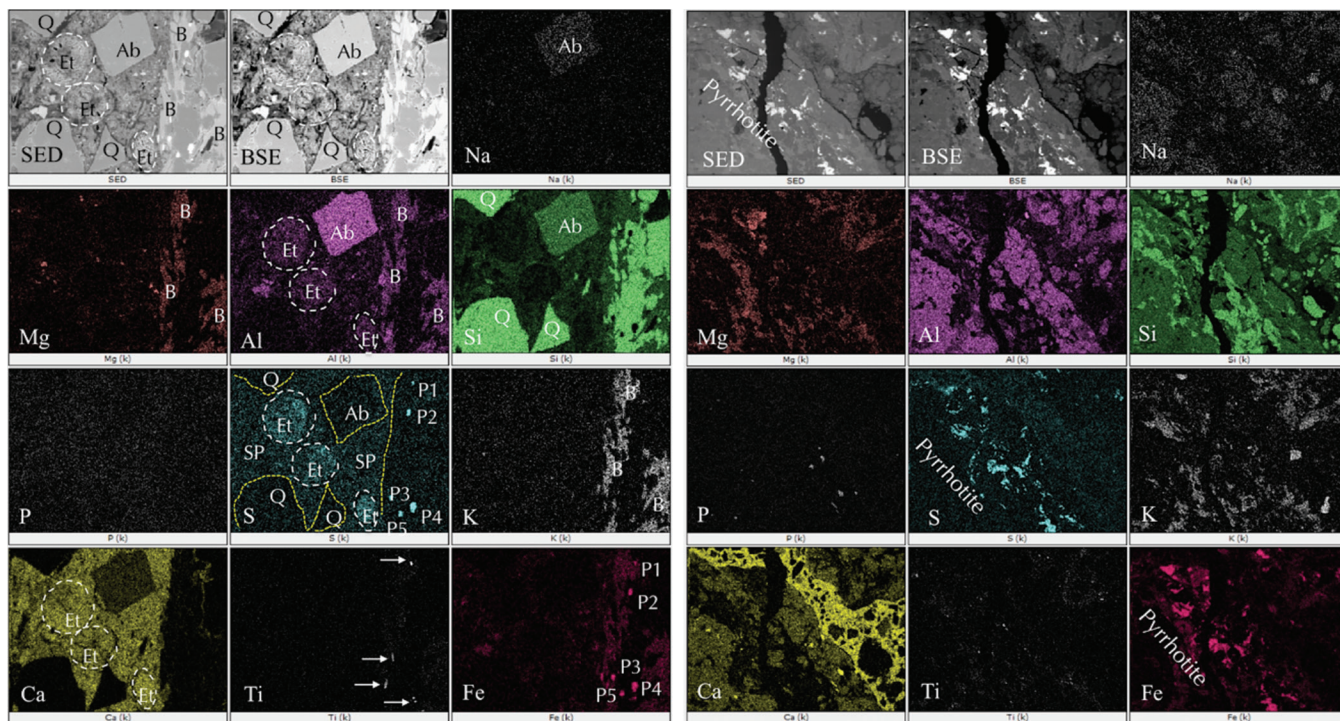


Fig. 10—Secondary electron image (SED), backscatter electron image (BSE), and X-ray elemental maps of sodium (Na), magnesium (Mg), aluminum (Al), silicon (Si), phosphorus (P), sulfur (S), potassium (K), calcium (Ca), titanium (Ti), and iron (Fe). Left set of maps show ettringite (Et)-filled air voids that are highlighted in Ca, Al, and S maps; biotite mica (B) is highlighted in K and Mg maps; albite feldspar (Ab) is highlighted in Si and Al maps; four fine-grained iron-titanium oxides are marked by arrows in Ti-map; fine pyrrhotite inclusions are highlighted as P1 through P5 in Fe, and S maps; and, most importantly, a sulfur-contaminated paste (marked SP in S-map) is showing S-signals stronger than the signals from aggregate areas but weaker than the signals from ettringite-filled voids. Right set of photos show pyrrhotite inclusions in gneiss that are highlighted in S and F maps. Ca-map between aggregates shows the typical calcium silicate hydrate composition of portland cement paste. Quartz (Q) and albitic feldspar (Ab) grains are highlighted in Si and Si-Al maps, respectively, whereas biotitic mica in gneiss is highlighted in K and Si maps.

9). Pyrrhotite content in the bulk concrete is 0.9%, whereas ferrihydrite content is 5.1% (Fig. 9).

SCANNING ELECTRON MICROSCOPY AND ENERGY-DISPERSIVE X-RAY MICROANALYSIS (SEM-EDS)

SEM-EDS studies found well-developed secondary ettringite crystallization mostly in air voids (Fig. 10) and only occasionally in microcracks, including in gaps around aggregates and at aggregate-paste interfaces (Fig. 11), which are more common microstructures of DEF-distressed concretes. Most of the microcracks are empty, and gaps around aggregates due to paste expansion are not as frequent as in DEF-affected concretes. However, EDS analyses of sulfate contents of paste are in the range of 4 to 6.5% (as SO_3 ; Fig. 11 and 12), which are noticeably higher than less than 1% sulfate (SO_3) commonly found in the paste of a normal portland-cement concrete prepared using a portland cement containing ~3% sulfate at a similar water-cement ratio (w/c) and cement content of the present concrete but containing no iron sulfide contaminant.

High sulfate content of paste, as detected from EDS analyses, is consistent with the ettringite-infested paste found in thin section photomicrographs during optical microscopy, as well as overall high bulk sulfate (SO_3) content of concrete,

indicating sulfate release from pyrrhotite oxidation. SEM-EDS analyses found three different optically opaque iron minerals in gneiss (Fig. 12)—for example, iron sulfide (pyrrhotite), oxidation products of pyrrhotite measured in the EDS as iron oxide (determined in XRD as ferrihydrite), and iron-titanium oxide (rutile and ilmenite). Some oxidized pyrrhotite grains show alternating sulfur-poor (oxygen-rich) oxidized bands and sulfur-rich (oxygen-poor) pyrrhotite bands, where iron content is higher in the oxidized bands (Fig. 13). The following chemical and microstructural features—high sulfate content of paste, detection of poorly crystalline ettringite-infested paste, high bulk sulfate content (1.45%) of concrete yet the absence of abundant secondary ettringite in many microcracks and gaps around aggregates except more profuse crystallization in air voids—indicate microcracking due to paste expansion by internal sulfate attack occurred from the development of poorly crystallized ettringite (and perhaps some in colloidal form) within the confined spaces in paste in the ettringite-infested regions, which are not always as frequently diagnosed as in DEF-affected concretes having well-crystallized delayed ettringite in cracks, gaps, and voids.

Therefore, this study showed clear microstructural evidence of: a) primary expansion of concrete due to oxidation of pyrrhotite in crushed gneiss coarse aggregate causing

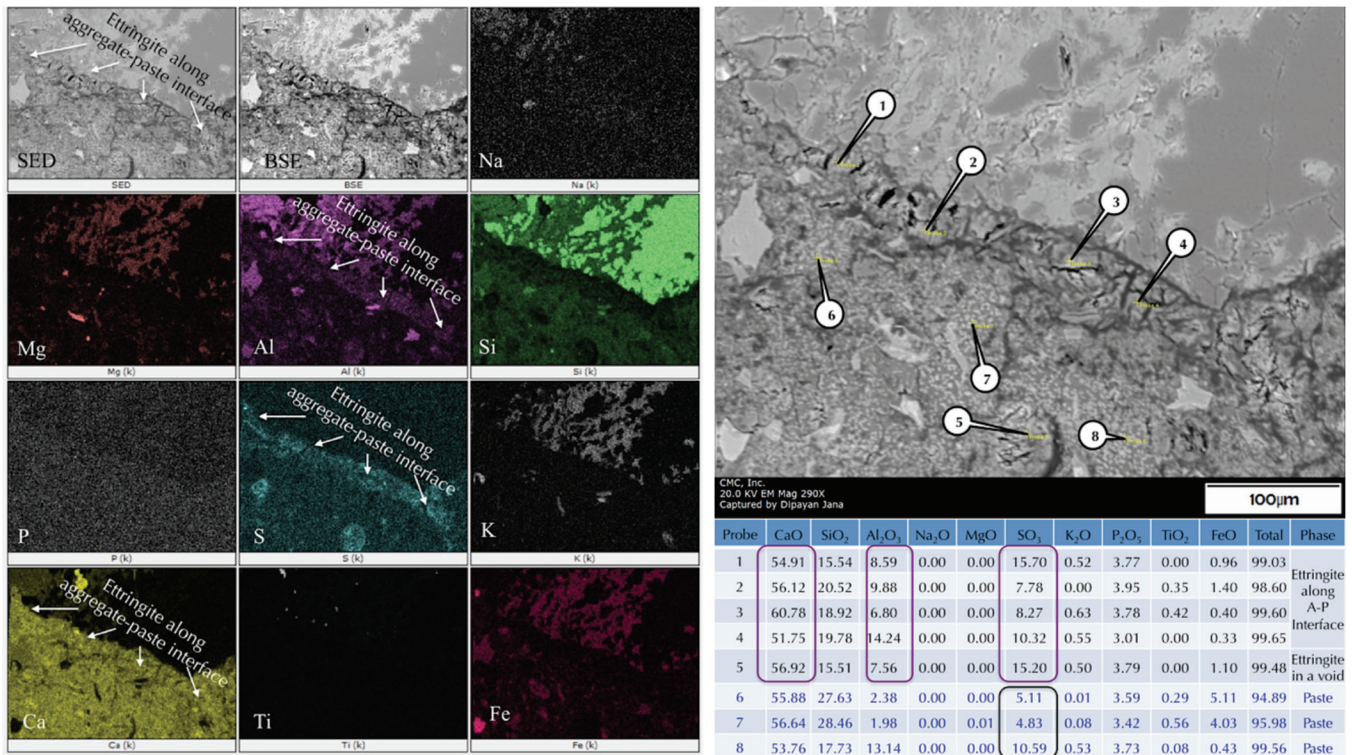


Fig. 11—X-ray elemental maps at left, secondary electron image at right and compositional analysis (oxide weight percentages) at the tips of callouts from various areas in paste and along aggregate-paste interface showing secondary ettringite formation at the interface as well as in the paste away from interface due to internal sulfate attack of sulfates released from pyrrhotite oxidation. Sulfate contents at the interfaces are noticeably higher due to profuse ettringite development (with characteristic Ca-S-Al enrichments in the respective maps shown by arrows) as opposed to a lower S-signal in the paste where ettringite is intermixed with other cement hydration products.

cracking within the unsound aggregate particles often extending into paste (mostly from optical microscopy); and b) secondary expansion of paste due to formation of poorly crystalline (perhaps also colloidal form) secondary ettringite in relatively confined areas in sulfate-contaminated ettringite-infested paste that are the breeding ground for internal sulfate attack causing paste expansion and associated cracking (from both optical and electron microscopy). Relatively well-developed secondary ettringite in voids and a few in cracks are judged to be the consequence of exposure of ettringite-infested paste to moisture during service, causing dissolution and reprecipitation of secondary ettringite in open spaces.

ACCELERATED OXIDATION AND ION CHROMATOGRAPHY

After the detection of pyrrhotite and its oxidation products, as well as evidences of internal sulfate attack in paste, a final piece of evidence is obtained from determining the amount and efficiency of release of sulfate from aggregates when exposed to a strong oxidizing solution, which is common in the high-pH environment of portland-cement concrete. In accelerated pyrrhotite oxidation test, multiple dark gray and light brown crushed gneiss coarse aggregate particles are extracted from the core, cleaned of adhered paste remains, crushed, and then immersed in a 35% hydrogen peroxide (strong oxidant) solution for several days.² Sulfates released from aggregates to the filtrates are measured (as SO₄²⁻) in an

anion exchange chromatograph. Two sets of each aggregate are measured for a 2-week period. A control gneiss sample from a different project without any iron sulfide mineral was also examined. All particles from the core show noticeable release of sulfates as opposed to no sulfate release from the control gneiss aggregate without pyrrhotite (Fig. 14).

AGGREGATE SCREENING AND PYRRHOTITE LIMIT

Standardization of the amount of iron sulfide minerals considered acceptable in concrete aggregates is not well established. American, Canadian, British, and French standards for concrete aggregates mention potential problems from use of iron sulfide in concrete but have not established acceptable limits of iron sulfide contents in aggregates. Limits have been established for total sulfur (S_T) by mass in French at 0.4%, and European at 1%, or 0.1% if pyrrhotite is present (NF EN 12620 “Aggregates for concrete,” and Annex P of CSA A23 “Concrete materials and methods of concrete construction/Test methods and standard practices for concrete”). The limits as to the amount of pyrrhotite that would lead to damage has not been identified to date; this may be quite difficult because the reactivity of pyrrhotite may vary according to its crystallographic characteristics, while many factors are involved in this deleterious mechanism. No precise guidelines or methods have been proposed at the time of this report to evaluate the potential reactivity of sulfide containing aggregates.

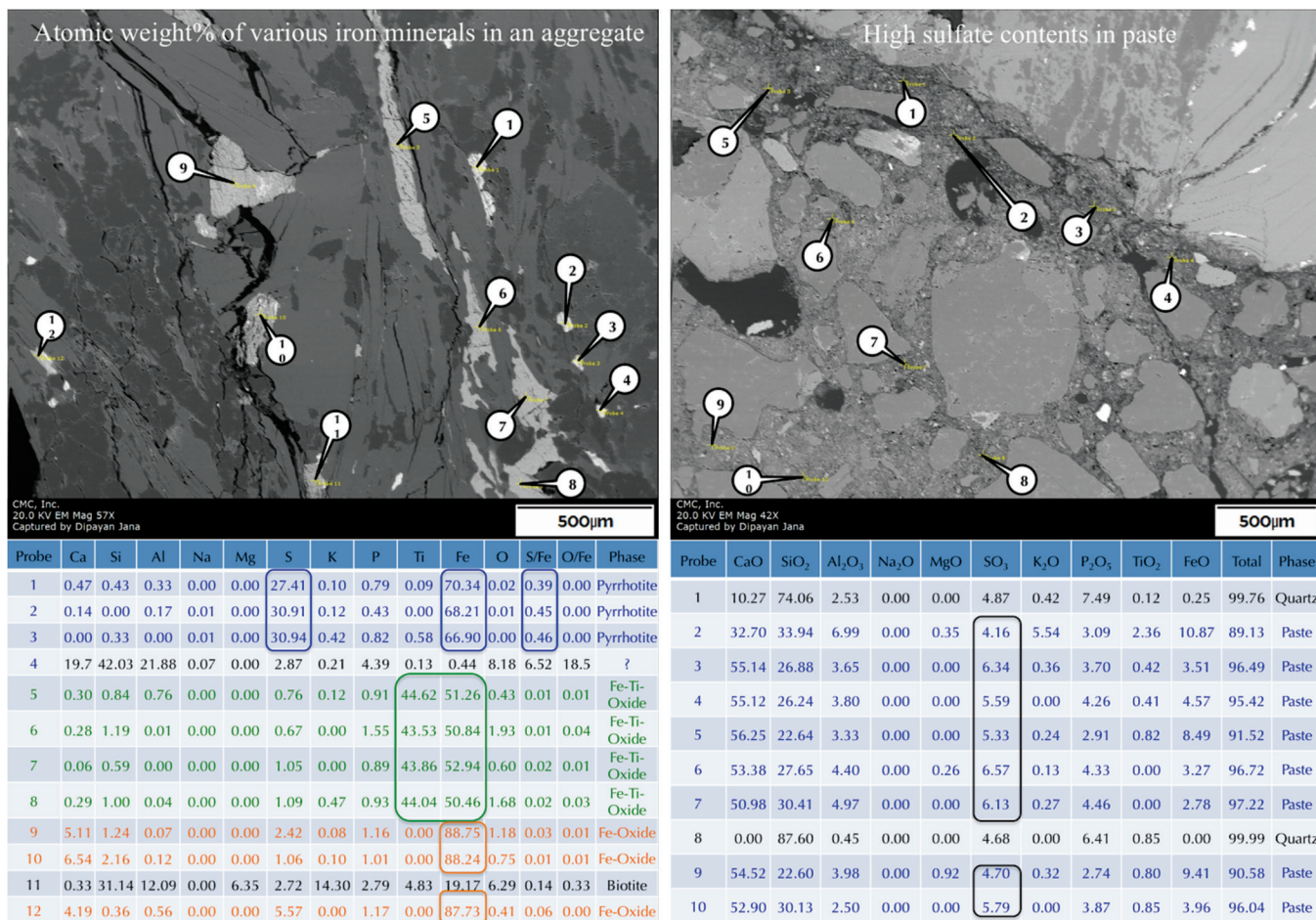


Fig. 12—Backscatter electron images and compositional analysis (oxide weight percentages) at the tips of callouts from various iron oxide and sulfide minerals in a coarse aggregate particle in the left, and from the paste regions in the right. Results of compositional analysis are derived from an energy-dispersive X-ray fluorescent spectrometer attached to a scanning electron microscope, which are given in the tables. Pyrrhotite, iron-titanium oxide, and iron oxide are the three common opaque phases present, of which pyrrhotite inclusions are distinguished by characteristic Fe, S, and S/Fe ratios. Paste in the right table shows characteristic enrichment in sulfur (as SO₃) from ettringite-infested paste due to internal sulfate attack, where SO₃ contents from 4 to 6% are significantly higher than that of a portland cement paste without any additional sulfur source than cement. Boxed areas in both tables highlight characteristic compositions of the phases of interest.

Recently, an extensive investigation was carried out over a 4-year period by researchers from four Canadian organizations aimed at developing an evaluation protocol for iron-sulfide-bearing aggregate.³¹ The resulting recommended protocol involved a three-phase testing program, including 1) measurement of total sulfur; 2) oxygen consumption determination; and 3) accelerated mortar bar expansion test. Limits are proposed for each phase of the protocol but need additional validation. The U.S. Army Corps of Engineers have proposed similar short- (1 to 2 years) to long-term (8+ years) testing protocols for aggregate regulations and structural assessments.³² Significant research is still needed to identify appropriate limits.

All testing protocols indicate additional evaluation of a quarry for use as concrete aggregate beyond the physical requirements and limits of potentially deleterious constituents mentioned in ASTM C33.³³ Figure 15 provides a five-step laboratory testing protocol of aggregates after found satisfactory according to ASTM C33 to further evaluate

any potentially deleterious reactions from oxidation of iron sulfide minerals, as follows:

1. Aggregates in conformance to the specification of ASTM C33³³ should be first examined by petrographic examinations (by ASTM C295³⁴), preferably on rock cores drilled from a quarry to represent different depths—for example, stratigraphic formations to examine the presence of iron sulfide minerals. Cores should be examined on cylindrical surfaces as well as on cross sections by using a low-power stereomicroscope, followed by preparing thin sections for further examinations in a petrographic microscope to determine the depth and abundance of various iron sulfide minerals.

2. Sulfur contents (as SO₃) of the portions of rock cores that have revealed the presence of iron sulfide minerals by petrography should then be determined by various chemical methods—for example, by portable handheld XRF on core sections, micro-XRF of core, benchtop ED-XRF on pressed pellets of pulverized rock, fused beads of pulverized rock in WD-XRF, or Leco combustion IR. A sulfur content of

less than 0.1% is usually considered as the safe limit for acceptance.³²

3. Aliquots of pulverized rocks used for chemical analyses should then be examined by X-ray diffraction (ASTM C1365²⁸) to determine the types and abundances of iron sulfide minerals, particularly pyrrhotite, as well as the oxidation products, if any.

4. Another aliquot of pulverized aggregate should be digested in a strong oxidizing solution of 35 to 40% hydrogen peroxide for several days to month for release of sulfates; the filtrate thus separated from oxidation, after appropriate dilution, should be tested by anion chromatography according to the methods of ASTM D4327²⁹ and Wille and Zhong² to determine the released sulfate level. Rodrigues et al.³⁵ suggested an oxygen consumption test to assess the oxidation potential of concrete aggregate, where a compacted layer of aggregate is exposed to oxygen (O₂) in a hermetic cell, and the O₂ consumption is monitored. Optimized parameters included a 10 cm compacted layer of aggregate material with particle size < 150 μm kept at 40% saturation degree with a 10 cm headspace left at the top of the cell. The consumption of the O₂ present in the headspace is monitored over a 3-hour testing period at 22°C; the test was able to discriminate sulfide-bearing aggregates from a control one when using a threshold limit of 5% O₂ consumed.

5. Aggregate that does not meet an acceptable criterion from the above four steps should finally be evaluated in a long-term accelerated mortar bar expansion test—for example, according to the methods of ASTM C157.³⁶ Rodrigues et al.³⁷ suggested 90 days of mortar bar storage at 80°C and 80% RH, with two 3-hour wetting cycles in a 6% bleach solution (Phase I) followed by up to 90 days of storage at 4°C and 100% RH (Phase II). Aggregates with an expansion over 0.15% during Phase I are rejected and thaumasite formation potential is detected by rapid regain of expansion followed by destruction of the samples during Phase II. The control aggregates without sulfide mineral did not show any signs of deterioration in either phases of the testing program.

Petrography, chemistry (total sulfur content), and XRD (pyrrhotite content) are the three primary tests needed for establishment of preliminary acceptance criteria prior to further verifications from accelerated oxidation and mortar bar expansion tests. A standardized limit on pyrrhotite content for acceptance or rejection as concrete aggregate can only be determined from such exercises encompassing microscopy, chemical, and mineralogical evaluations.

DISCUSSIONS

Iron sulfide minerals are unstable in oxidizing conditions causing ready oxidation and release of sulfates. High pH conditions, such as those found in concrete, enhance iron sulfide oxidation. Upon exposure to water and oxygen, sulfide minerals (pyrite, pyrrhotite) oxidize to form acidic, iron oxides/hydroxides/oxyhydroxides, and sulfate-rich by-products with an increase in solid volumes from the sulfide minerals to their oxidized products.^{21,38-40} The oxidation of ferrous iron (Fe²⁺) produces ferric ions (Fe³⁺) that can precipitate out of solution to form ferric hydroxide, if pH is not too low. Fe²⁺ is oxidized and precipitated as ferric

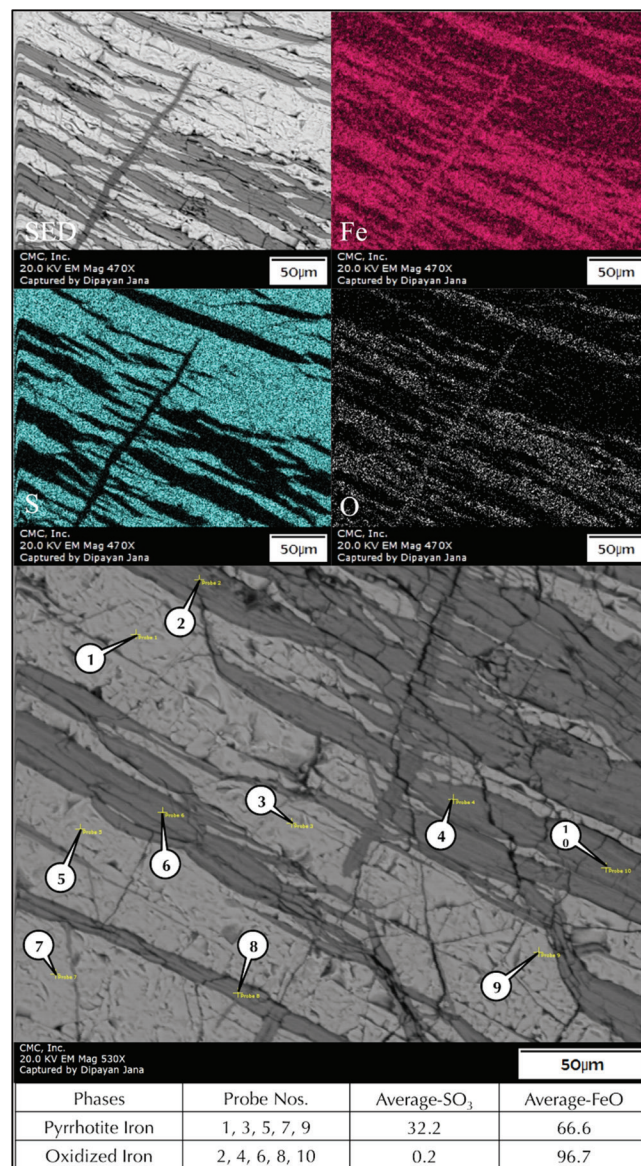


Fig. 13—Elemental maps of iron (Fe), sulfur (S), and oxygen (O) in an oxidized pyrrhotite grain showing alternating S-poor (O-rich) oxidized bands and S-rich (O-poor) pyrrhotite bands. Iron contents are higher in the oxidized bands than in the pyrrhotite bands. A crack transecting the alternating bands is filled with oxidized iron. Bottom secondary electron image shows average compositional analyses (oxide weight percentages) of oxidized iron and pyrrhotite bands.

oxyhydroxides, principally ferrihydrite [Fe(OH)₃] and goethite [FeO(OH)]. The sulfuric acid (sulfate and hydrogen ion [H₂SO₄]) generated through oxidation reactions reacts with cement hydration products, for example, with portlandite [Ca(OH)₂] to form gypsum [CaSO₄·2H₂O],^{20,21,41,42} with calcium aluminate or monosulfoaluminate hydrates to form ettringite [Ca₆Al₂(SO₄)₃(OH)₁₂·26H₂O] or thaumasite [Ca₆[Si(OH)₆]₂(CO₃)₂(SO₄)₂(H₂O)₂₂—the latter if carbonate minerals are present. Both the processes of oxidation of iron sulfides and reactions between released sulfates and cement hydration products are quite expansive in nature, resulting in concrete deteriorations.

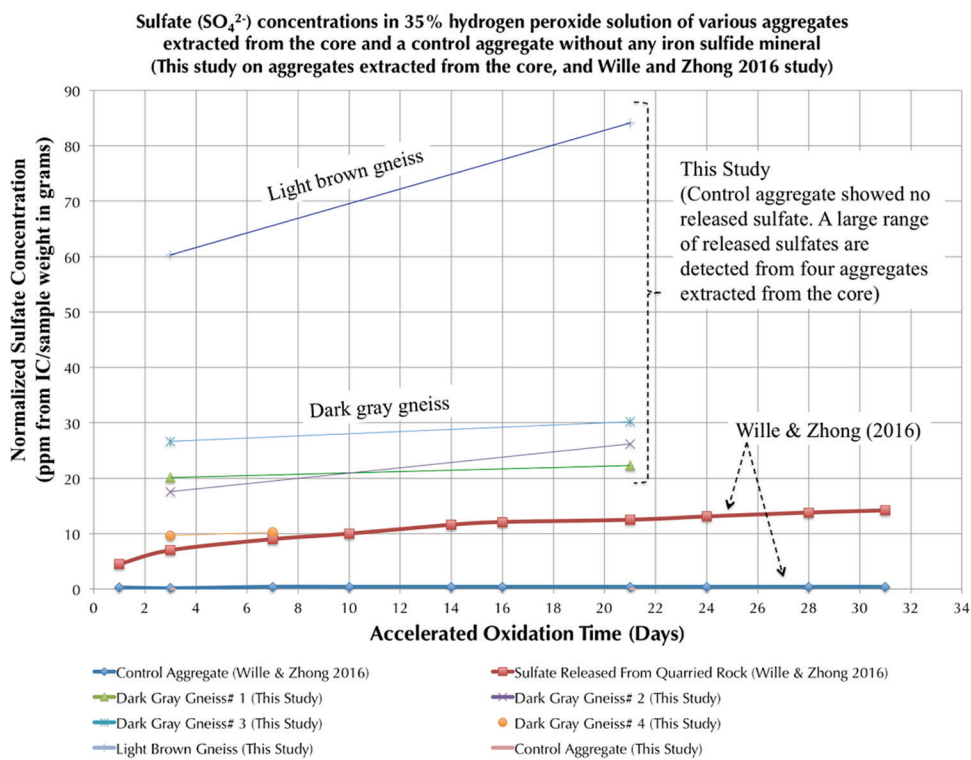
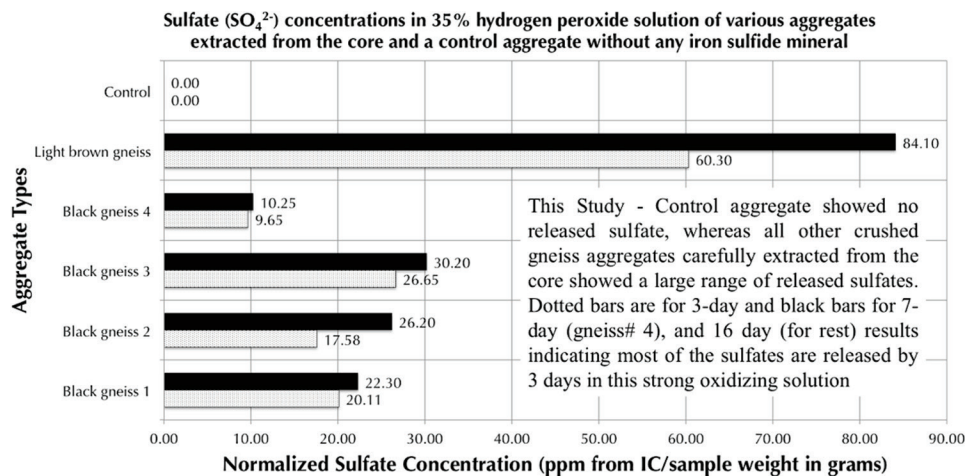


Fig. 14—Determination of amount of sulfate released from accelerated oxidation test of crushed gneiss aggregates extracted from the core, immersed in a 35% hydrogen peroxide solution for 3 to 16 days, then filtered through 25 micron filter papers, diluted, and analyzed in an ion chromatogram. Results show increasing sulfate release from all aggregate particles, as also seen in the study of Willi and Zhong,² and highest sulfate release in a light brown gneiss.

Figure 1 from various authors^{2,12,21} summarizes mechanisms of two-stage expansions resulting in concrete deterioration from: a) primary expansion due to oxidation of iron sulfide minerals to ferric oxyhydroxides, principally goethite and ferrihydrite and associated solid volume increase; and b) secondary expansion due to internal sulfate attacks of released sulfate and hydrogen ions (sulfuric acid) from oxidation to cement hydration products—for example, calcium hydroxide and calcium sulfoaluminate hydrate to form gypsum (with a solid volume increase of 42 cm³/mole of sulfide²) or more commonly due to formation of ettringite (with a solid volume increase of 172 cm³/mole of sulfide²). The above expansive mineral formation results in rust staining and popouts at the aggregate site in milder cases most commonly associated with pyrite, to severe cracking and decreased strength due to

internal sulfate attack in paste from released sulfates in the most severe cases associated with pyrrhotite.

In the case of pyrrhotite, the degree of damage correlates with the deterioration of the mineral and the quantity of resultant expansive sulfates in the paste. However, not all concretes with pyrrhotite in aggregates result in deterioration. As shown in the case studies in Table 1, the rate and extent of damage can be variable. The rate and severity of damage are dependent on a number of factors, including: a) the interaction between the particle and the surrounding host rock that forms the aggregate¹² and the concrete paste; b) the concrete quality; c) the environmental conditions to which the concrete element is exposed to (exposure to oxygen, moisture, and temperature); d) crystal structure; e) the mineral associations (more than one sulfide mineral

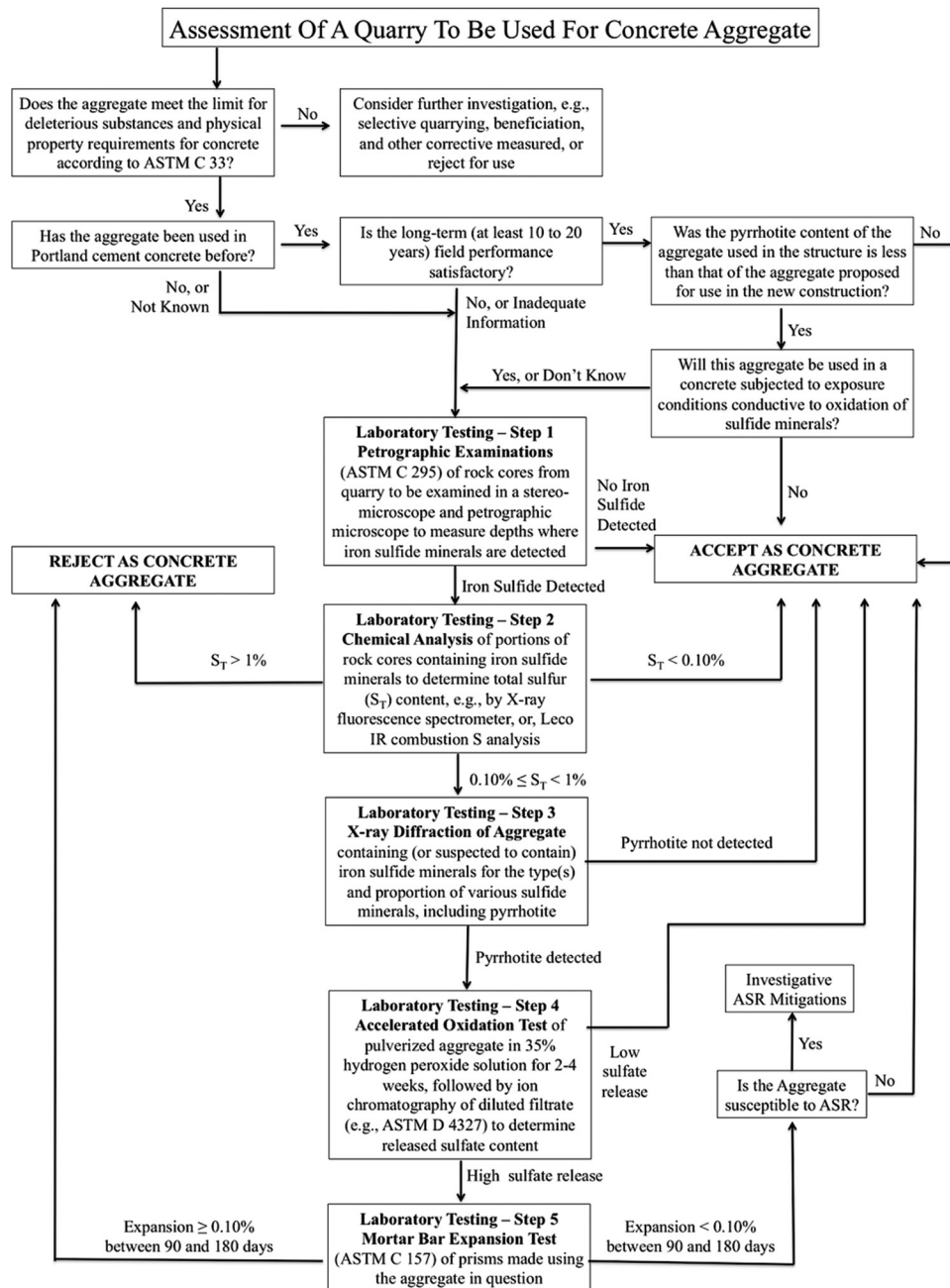


Fig. 15—Assessment of a quarry through five-step laboratory testing protocol for use as concrete aggregate to mitigate pyrrhotite-related deterioration (modified from Rodrigues et al.³¹ and Moore et al.³²).

present); f) concrete pH; g) trace metal content; and h) bacterial activity.³⁸ The extents of controlling factors are not yet fully understood in light of the limitations of reproducing the deterioration in the laboratory.

CONCLUSIONS

Laboratory studies on numerous pyrrhotite-related concrete deteriorations from various foundation walls in the eastern Connecticut region have led to the following conclusions:

1. Cracking and crumbling of concrete foundation walls are due to oxidation of unsound pyrrhotite grains in crushed gneiss coarse aggregate from Becker's quarry in Wilmington, CT in the presence of oxygen and moisture during service in concrete. Cracking provides pathways for continued migra-

tion of moisture and oxygen into the walls and, therefore, continued distress.

2. The host rock for pyrrhotite mineralization used as coarse aggregate in concrete is the predominantly dark gray garnetiferous quartz-feldspar-biotite gneiss having alternating bands of quartz-feldspar and micaceous (mostly biotite) minerals and garnet poikiloblast and lesser amounts of light brown gneiss having more quartz and less pyrrhotite than the dark gray stones. Amount of pyrrhotite grains, however, varied widely among different crushed gneiss particles, irrespective of the host rock mineralogy.

3. Sulfur (as SO₃) contents in the pyrrhotite-bearing crushed gneiss aggregates are from 2% in light brown gneiss to as high as 10% in predominant dark gray gneiss particles, or perhaps even higher, giving a total bulk sulfate

(SO₃) content of 1.45% in the concrete, which is more than three times the sulfate in a normal portland-cement concrete without any iron sulfide contaminant. As high as 8% pyrrhotite is found from XRD analysis of dark gray gneiss, indicating significant pyrrhotite mineralization in the gneiss used as coarse aggregate.

4. Oxidation of pyrrhotite has formed ferrihydrite with an expansion of unsound crushed gneiss coarse aggregate, causing extensive cracking in many particles having cracks extending from the affected particles to paste. The typical gneissose texture of quarried aggregates has facilitated crack formation during expansion due to the presence of inherent planes of weakness along the micaceous bands in gneiss. Reddish brown rust stains found in many distressed foundations are due to pyrrhotite oxidation and formation of iron oxy-hydroxides (for example, goethite and limonite) and ferrihydrites.

5. Evidence of pyrrhotite oxidation is confirmed from: a) detection of ferrihydrite in XRD, and b) from SEM-EDS studies of lower than stoichiometric S/Fe ratio of many pyrrhotite grains (mostly <0.50), indicating advanced oxidation. Microstructural evidence of oxidation-related expansion of unsound aggregate is found from extensive cracking of many of these crushed gneiss coarse aggregate particles often extending into the paste.

6. Pyrrhotite oxidation has readily released sulfates and contaminated the portland cement paste as detected from high (4 to 6.5%) sulfate contents in the SEM-EDS analyses of paste as opposed to normal less than 1% sulfate found in the paste of a portland-cement concrete containing no iron sulfide contaminants. Ready release of sulfate has promoted internal sulfate attack and subsequent secondary expansion of paste with additional cracking.

7. To determine effectiveness of sulfate release in an oxidizing environment, crushed gneiss coarse aggregates subjected to a strong oxidizing solution (of 35% hydrogen peroxide) showed significant release of sulfate, mostly within 3 days of immersion, even after decades of service in the concrete. The amount of sulfate release depends on the mineralogy (for example, pyrrhotite content) of crushed gneiss.

8. Sulfates released from pyrrhotite oxidation have reacted with cement hydration products and formed poorly crystallized (or perhaps some colloidal form) secondary ettringite within the confined spaces in paste with the resultant secondary expansion of paste and additional cracking within the paste and around aggregate-paste interfaces. Presence of excess sulfates, moisture, and open spaces of air voids and cracks have facilitated dissolution and precipitation of well-crystallized fibrous secondary ettringite in voids and occasionally in cracks that were visible in optical microscopy and SEM analyses.

9. Evidence of internal sulfate attack in paste came first from the paste chemistry—that is, a) very high sulfate (SO₃) content of paste from SEM-EDS studies, and then from various microstructural evidences in optical and scanning electron microscopy; b) ettringite-infested paste containing poorly crystalline (perhaps some colloidal) form of ettringite; c) well-formed secondary ettringite crystallization

in aggregate-paste interfaces, microcracks, and air voids, often due to moisture-induced dissolution of ettringite from ettringite-infested confined areas of paste and precipitation of relatively well-formed ettringite in voids and cracks; and d) gaps between aggregates due to expansion of paste (more common in many other concrete distresses due to internal sulfate attack than the present one).

10. Relative roles of primary expansion of unsound aggregates due to pyrrhotite oxidation and secondary expansion of paste due to internal sulfate attack on the overall distress of foundation depend on various factors—for example, proportion of pyrrhotite (and total available sulfate), moisture condition during service, consolidation, and degree of impermeability of concrete to moisture ingress.

11. In light of the observed severe cracking of the foundation wall all throughout the thickness, and its anticipated progress with potential worsening of condition with time, replacement of the wall is the only viable option with particular emphasis to avoid use of aggregate from the subject quarry or elsewhere that contains pyrrhotite, let alone anywhere near the amount that have caused cracking.

12. Due to the known geology of extensive pyrrhotite mineralization in the hydrothermal vein in which the quarry reportedly supplied the unsound aggregate for concrete in thousands of homes in Connecticut, aggregates for new construction in the neighborhood should be evaluated for the possible presence of pyrrhotite from petrography, sulfur content (XRF), mineralogy (XRD), and effectiveness of sulfate release in an oxidizing environment (from accelerated oxidation test). All these tests can be done in short-term (within weeks to a month) tests as opposed to long-term tests—for example, an accelerated mortar bar expansion test for 3- to 6-month period.

13. Because there is no industry specification on the threshold pyrrhotite limit above which potential for oxidation-related distress can occur⁴³—in fact, as low as 0.3% pyrrhotite by mass of aggregate in the host rock has reportedly shown severe distress in concrete (for example, in Quebec, Canada⁴)—the best solution is to avoid aggregates containing pyrrhotite for its known deleterious effects, or use aggregate having less than 0.10% sulfur or set the sulfur limit based on the type of iron sulfide mineral present.⁴⁴ Effective sealing of foundation walls (and existing cracks as soon as observed) to prevent moisture ingress could also reduce future deterioration.

AUTHOR BIOS

ACI member Dipayan Jana is the President of Construction Materials Consultants, Inc. and Applied Petrographic Services, Inc., Registered Professional Geologist in Washington and Texas. He received his BSc, MSc, and MS in geology, and was in the doctoral program from University of Calcutta, India, University of Illinois at Chicago, Chicago, IL, and Columbia University, New York, in 1987, 1989, 1993, and 1996, respectively. He is a member of ACI Committees 201, Durability of Concrete, and 221, Aggregates. His research interests include microstructural analysis for assessment of durability of reinforced concrete structures.

ACKNOWLEDGMENTS

Sincere thanks to D. H. Campbell for a thorough review and comments on the manuscript. J. Hall is acknowledged for review and editing of the manuscript.

REFERENCES

1. Deer, W. A.; Howie, R. A.; and Zussman, J., *An Introduction to the Rock-Forming Minerals 3rd Edition*, Berforts Information Press, UK, 2013, 696 pp.
2. Wille, K., and Zhong, R., "Investigating the Deterioration of Basement Walls Made of Concrete in CT," *Report for the Attorney General of the State of Connecticut*, University of Connecticut, Storrs, CT, 2016, 93 pp.
3. Moum, J., and Rosenqvist, I. T. "Sulfate Attack on Concrete in the Oslo Region," *ACI Journal Proceedings*, V. 56, No. 18, 1959, pp. 257-264.
4. Tagnit-Hamou, A.; Saric-Coric, M.; and Rivard, P. "Internal Deterioration of Concrete by Oxidation of Pyrrhotitic Aggregates," *Cement and Concrete Research*, V. 35, No. 1, 2005, pp. 99-107. doi: 10.1016/j.cemconres.2004.06.030
5. Rodgers, J., "Bedrock Geological Map of Connecticut," Connecticut Geological and Natural History Survey, 1985.
6. Duchesne, J., and Benoit, F. "Deterioration of Concrete by the Oxidation of Sulphide Minerals in the Aggregate," *Journal of Civil Engineering and Architecture*, V. 7, No. 8, 2013, pp. 922-931.
7. Duchesne, J., and Fournier, B., "Petrography of Concrete Deteriorated by Weathering of Sulphide Minerals," International Cement Microscopy Association Conference, Apr. 2011.
8. Araujo, G. S.; Chinchon, J. S.; and Aguado, A. "Evaluation of the Behavior of Concrete Gravity Dams Suffering from Internal Sulfate Attack," *IBRACON Structures and Materials Journal*, V. 1, No. 1, July 2008, pp. 84-112.
9. Chinchón, J. S.; Ayora, C.; Aguado, A.; and Guirado, F. "Influence of Weathering of Iron Sulfides Contained in Aggregates on Concrete Durability," *Cement and Concrete Research*, V. 25, No. 6, 1995, pp. 1264-1272. doi: 10.1016/0008-8846(95)00119-W
10. Chinchón-Payá, S.; Aguado, A.; and Chinchon, S. "A Comparative Investigation of the Degradation of Pyrite and Pyrrhotite Under Simulated Laboratory Conditions," *Engineering Geology*, V. 127, 2012, pp. 75-80. doi: 10.1016/j.enggeo.2011.12.003
11. Ayora, C.; Chinchon, J. S.; Aguado, A.; and Guirado, F. "Weathering of Iron Sulfides and Concrete Alteration: Thermodynamic Model and Observation in Dams from Central Pyrenees, Spain," *Cement and Concrete Research*, V. 28, No. 9, 1998, pp. 1223-1235. doi: 10.1016/S0008-8846(98)00137-9
12. Oliveira, I.; Cavalaro, S. H. P.; and Arguado, A. "Evolution of Pyrrhotite Oxidation in Aggregates for Concrete," *Materiales de Construcción*, V. 64, No. 316, 2014, pp. 1-10.
13. Quigley, R. M., and Vogan, R. W. "Black Shale Heaving at Ottawa, Canada," *Canadian Geotechnical Journal*, V. 7, No. 2, 1970, pp. 106-112. doi: 10.1139/t70-012
14. Bérard, J. "Black Shale Heaving at Ottawa, Canada: Discussion," *Canadian Geotechnical Journal*, V. 7, No. 2, 1970, pp. 113-114. doi: 10.1139/t70-013
15. Bérubé, M.-A.; Locat, J.; Gélinas, P.; Chagnon, J.-Y.; and Lefrançois, P. "Black Shale Heaving at Sainte-Foy, Quebec, Canada," *Canadian Journal of Earth Sciences*, V. 23, No. 11, 1986, pp. 1774-1781. doi: 10.1139/e86-163
16. Penner, E.; Eden, W. J.; and Grattan-Bellew, P. E., "Expansion of Pyritic Shales," CBD-152, Canadian Building Digest, National Research Council, Canada, 1972, 6 pp.
17. Hawkins, A. B., and Pinches, G. M. "Cause and Significance of Heave at Llandough Hospital, Cardiff - A Case History of Ground Floor Heave due to Gypsum Growth," *Quarterly Journal of Engineering Geology and Hydrogeology*, V. 20, No. 1, 1987, pp. 41-57. doi: 10.1144/GSL.QJEG.1987.020.01.05
18. Hoover, S. E., and Lehmann, D. "The Expansive Effects of Concentrated Pyritic Zones within the Devonian Marcellus Shale Formation of North America," *Quarterly Journal of Engineering Geology and Hydrogeology*, V. 42, No. 2, 2009, pp. 157-164. doi: 10.1144/1470-9236/07-086
19. Anderson, W.H. "Foundation Problems and Pyrite Oxidation in the Chattanooga Shale," *Report of Investigations 18*, Geological Survey Report of Investigation, Estill County, KY, 2008.
20. Shayan, A. "Deterioration of a Concrete Surface Due to the Oxidation of Pyrite Contained in Pyritic Aggregate," *Cement and Concrete Research*, V. 18, No. 5, 1988, pp. 723-730. doi: 10.1016/0008-8846(88)90095-6
21. Rodrigues, A.; Duchesne, J.; Fournier, B.; Durand, B.; Rivard, P.; and Shehata, M. "Mineralogical and Chemical Assessment of Concrete Damaged by the Oxidation Of Sulfide-Bearing Aggregates: Importance of Thaumassite Formation on Reaction Mechanisms," *Cement and Concrete Research*, V. 42, No. 10, 2012, pp. 1336-1347. doi: 10.1016/j.cemconres.2012.06.008
22. Holleran, L., "Crumbling Foundations," Connecticut Department of Housing, Hartford, CT, Dec. 2018.
23. Mahoney, J. "Aggregates Containing Pyrrhotite," presentation, Connecticut Transportation Institute.
24. Connecticut Geological and Natural History Survey, DEP, in cooperation with the U.S. Geological Survey, "Bedrock Geology of Connecticut," Sept. 18, 2003. http://magic.lib.uconn.edu/cgi-bin/MAGIC_DBsearch2.pl?Geography=37800&Loc=0000.
25. Capitol Region Council of Governments (CRCOG). "Crumbling Foundations," 2016, <http://crocog.org/wp-content/uploads/2016/07/Crumbling-Foundations-presentation-July-25-Final.pptx>
26. ASTM C856-14, "Standard Practice for Petrographic Examination of Hardened Concrete," ASTM International, West Conshohocken, 2014, 17 pp.
27. ASTM C1723-16, "Standard Guide for Examination of Hardened Concrete Using Scanning Electron Microscopy," ASTM International, West Conshohocken, PA, 2016, 9 pp.
28. ASTM C1365-18, "Standard Test Method for Determination of the Proportion of Phases in Portland Cement and Portland-Cement Clinker Using X-Ray Powder Diffraction Analysis," ASTM International, West Conshohocken, PA, 2018, 11 pp.
29. ASTM D4327-17, "Standard Test Method for Anions in Water by Suppressed Ion Chromatography," West Conshohocken, PA, ASTM International, 2017, 13 pp.
30. Jana, D., "DEF and ASR in Concrete—A Systematic Approach from Petrography," *Proceedings of the 30th Conference on Cement Microscopy*, ICMA, Reno, NV, 2008.
31. Rodrigues, A.; Duchesne, J.; Fournier, B.; Durand, B.; Shehata, M.; and Rivard, P. "Evaluation Protocol for Concrete Aggregates Containing Iron Sulfide Minerals," *ACI Materials Journal*, V. 113, No. 3, 2016, pp. 349-359. doi: 10.14359/51688828
32. Moore, C.M., Strack, C.M., Moser, R.D., and McMahon, G.W. "Proposed Testing and Research Approach for Pyrrhotite-Induced Concrete Deterioration," Engineer Research and Development Center (ERDC), U.S. Army Corps of Engineers, Washington, DC, Oct. 2018.
33. ASTM C33/C33M-18, "Standard Specification for Concrete Aggregate," ASTM International, West Conshohocken, PA, 2018, 8 pp.
34. ASTM C295/C295M-18, "Standard Guide for Petrographic Examination of Aggregates for Concrete," ASTM International, West Conshohocken, PA, 2018, 9 pp.
35. Rodrigues, A.; Duchesne, J.; and Fournier, B. "Quantitative Assessment of the Oxidation Potential of Sulfide-Bearing Aggregates in Concrete Using an Oxygen Consumption Test," *Cement and Concrete Composites*, V. 67, 2016, pp. 93-100. doi: 10.1016/j.cemconcomp.2016.01.003
36. ASTM C157/C157M-17, "Standard Test Method for Length Change of Hardened Hydraulic-Cement Mortar and Concrete," ASTM International, West Conshohocken, PA, 2017, 8 pp.
37. Rodrigues, A.; Duchesne, J.; and Fournier, B. "A New Accelerated Mortar Bar Test to Assess the Potential Deleterious Effect of Sulfide-Bearing Aggregate in Concrete," *Cement and Concrete Research*, V. 73, 2015, pp. 96-110. doi: 10.1016/j.cemconres.2015.02.012
38. Belzile, N.; Chen, Y.-W.; Cai, M.-F.; and Li, Y. "A Review on Pyrrhotite Oxidation," *Journal of Geochimical Exploration*, V. 84, No. 2, 2004, pp. 65-76. doi: 10.1016/j.gexplo.2004.03.003
39. Casanova, I.; Aguado, A.; and Agullo, L. "Aggregate Expansivity Due to Sulfide Oxidation—II, Physico-Chemical Modeling of Sulfate Attack," *Cement and Concrete Research*, V. 27, No. 11, 1997, pp. 1627-1632. doi: 10.1016/S0008-8846(97)00148-8
40. Casanova, I.; Agullo, L.; and Aguado, A. "Aggregate Expansivity Due to Sulfide Oxidation—I, Reaction System and Rate Model," *Cement and Concrete Research*, V. 26, No. 7, 1996, pp. 993-998. doi: 10.1016/0008-8846(96)00085-3
41. Jana, D., "Concrete Deterioration from Pyrite Staining, Sewer Gases, and Chimney Flue Gases - Case Studies Showing Microstructural Similarities," *Proceedings of the 30th Conference on Cement Microscopy*, ICMA, Reno, NV, 2008.
42. Grattan-Bellew, P. E., and Eden, W. J. "Concrete Deterioration and Floor Heave Due to Biogeochemical Weathering of Underlying Shale," *Canadian Geotechnical Journal*, V. 12, No. 3, 1975, pp. 372-378. doi: 10.1139/t75-041
43. ACI Committee 201, "Guide to Durable Concrete (ACI 201.2R-08)," American Concrete Institute, Farmington Hills, MI, 2008, 49 pp.
44. Marcelino, A. P.; Calixto, J. M.; Gumieri, A. G.; Ferreira, M. C.; Caldeira, C. L.; Silva, M. V.; and Costa, A. L. "Evaluation of Pyrite and Pyrrhotite in Concretes," *IBRACON Structures and Materials Journal*, V. 9, No. 3, 2016, pp. 1-10.

NOTES:
